

Origin and morphology of limestone caves

ARTHUR N. PALMER *Department of Earth Sciences, State University of New York, College at Oneonta, Oneonta, New York 13820-4015*

ABSTRACT

Limestone caves form along ground-water paths of greatest discharge and solutional aggressiveness. Flow routes that acquire increasing discharge accelerate in growth, while others languish with negligible growth. As discharge increases, a maximum rate of wall retreat is approached, typically about 0.01–0.1 cm/yr, determined by chemical kinetics but nearly unaffected by further increase in discharge. The time required to reach the maximum rate is nearly independent of kinetics and varies directly with flow distance and temperature and inversely with initial fracture width, discharge, gradient, and P_{CO_2} . Most caves require 10^4 – 10^5 yr to reach traversable size. Their patterns depend on the mode of ground-water recharge. Sinkhole recharge forms branching caves with tributaries that join downstream as higher-order passages. Maze caves form where (1) steep gradients and great undersaturation allow many alternate paths to enlarge at similar rates or (2) discharge or renewal of undersaturation is uniform along many alternate routes. Flood water can form angular networks in fractured rock, anastomotic mazes along low-angle partings, or sponge-work where intergranular pores are dominant. Diffuse recharge also forms networks and sponge-work, often aided by mixing of chemically different waters. Ramiform caves, with sequential outward branches, are formed mainly by rising thermal or H_2S -rich water. Dissolution rates in cooling water increase with discharge, CO_2 content, temperature, and thermal gradient, but only at thermal gradients of more than 0.01 °C/m can normal ground-water CO_2 form caves without the aid of hypogenic acids or mixing. Artesian flow has no inherent tendency to form maze caves. Geologic structure and stratigraphy influence cave orientation and extent, but alone they do not determine branch-work versus maze character.

INTRODUCTION

Karst landscapes, in which dissolution of bedrock by water is one of the dominant geomorphic processes, occupy ~10%–20% of the Earth's land area. Nearly all major surface karst features owe their origin to internal drainage, subsidence, and collapse triggered by the development of underlying caves. An understanding of cave development is essential to the hydrologic or geomorphic interpretation of any karst region, and in assessing aquifer yield, contaminant migration, and soil and bedrock stability. Dissolution processes are also important to such topics as carbonate diagenesis, the origin of petroleum reservoirs, and the emplacement of hydrothermal ores.

In the past few decades, the amount of field and laboratory data related to limestone caves has increased enormously. Caves have been interpreted in terms of ground-water chemistry and hydrology (Thraill, 1968), geomorphic setting and lithology (Powell, 1970), aquifer type (White, 1969, 1977a), geologic structure (Ford, 1971), potential fields (Ewers, 1978; Ford and Ewers, 1978), hydraulics and geologic structure (Palmer, 1975), and solution kinetics (White, 1977b; Palmer, 1981, 1984a; Dreybrodt, 1981a, 1981b, 1987, 1988). Broad reviews of the subject have been given by Jennings (1985), White (1988), and Ford and Williams (1989).

This paper focuses on the origin of the basic cave patterns and on rates of cave enlargement. Coverage is limited to the solutional origin of caves in carbonate rocks, particularly limestones. Cave deposits are discussed only where they relate to cave origin. Although much of this paper is analytical, its conclusions are supported by previous field work in ~500 caves in all common geomorphic settings (see Palmer, 1975, 1984a, 1987). This information is supplemented by published data on several thousand other caves. Weighted by length, the relative frequency of major cave patterns in the investigated sample matches, within 1%, that of all

known caves in the world more than 3 km long (Courbon and Chabert, 1986); therefore, this sample is representative of all major solutional caves.

CAVE MORPHOLOGY

Pre-Solutional Openings

Solutional caves form where there is enough subsurface water flow to remove dissolved bedrock and keep undersaturated water in contact with the soluble walls. This is possible only where a pre-existing network of integrated openings connects the recharge and discharge areas. Of the total length of cave passages in the observed sample, 57% were guided by favorable beds or bedding-plane partings, 42% by prominent fractures, and only 1% by intergranular pores.

Passages influenced by bedding-plane partings are sinuous and curvilinear (Figs. 1a and 1c). Closely spaced joints within favorable beds may produce a similar pattern (Powell, 1976). Solutionally enlarged joints and high-angle faults tend to produce fissure-like passages with lenticular cross sections and angular intersections. Where joints are prominent, they can determine the pattern of nearly every passage in a cave (Fig. 1b). Faults usually exert only local control of cave passages and determine the overall trend of relatively few caves (Kastning, 1977). Intergranular pores are significant to cave origin only in reef limestones and poorly lithified grainstones.

Cave Patterns

All but the simplest caves consist of arrays of intersecting passageways that form distinctive patterns (Fig. 1). The fundamental pattern of a cave can be identified from field observation or plan-view maps, unless too little of the cave is accessible. Different parts of the same cave may possess different patterns, and more than one pattern can be superposed in a single location.

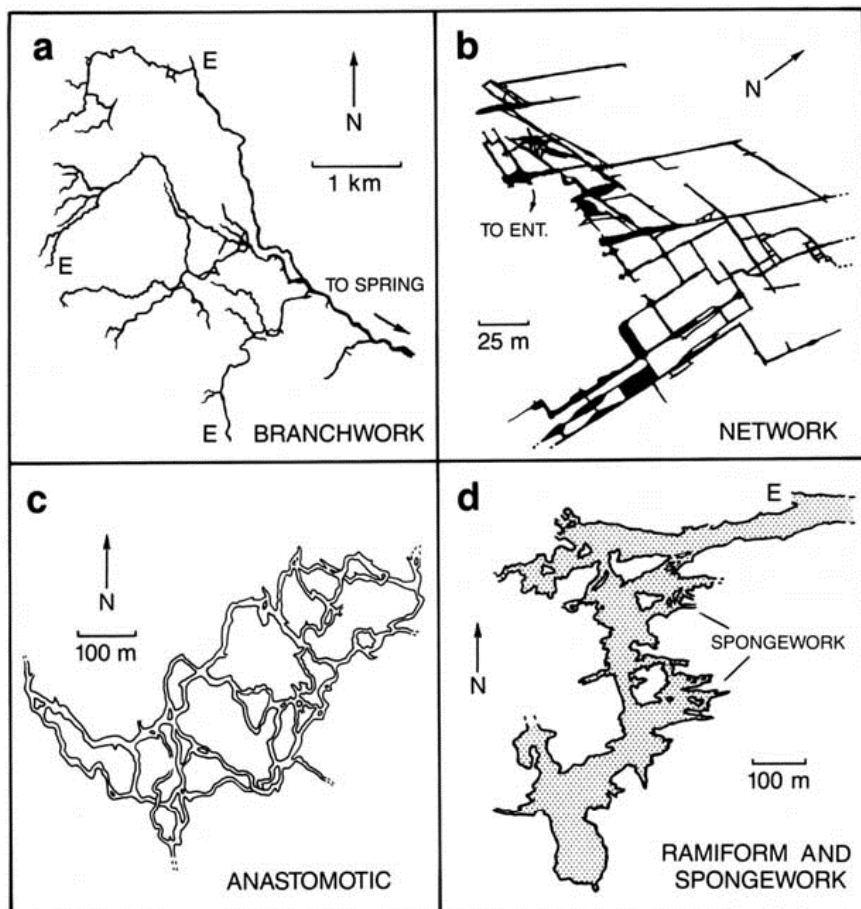


Figure 1. Common patterns of solutional caves: (a) branchwork: Crevice Cave, Missouri (Joachim Fm.); (b) network: part of Crossroads Cave, Virginia (New Scotland Fm.), (c) anastomotic: part of Hölloch, Switzerland (Cretaceous Schrattenkalk), (d) ramiform and spongework: Carlsbad Cavern, New Mexico (Capitan Fm.). E = entrance. Because of their small width-to-length ratio, passages in a and b are shown as solid lines. Maps reproduced with permission of (a) Paul Hauck, (b) H. H. Douglas, (c) Alfred Bögli, (d) Cave Research Foundation.

Branchwork caves consist of passages that join as tributaries (Figs. 1a and 2). They are by far the most common type, representing 57% of the caves observed for this study and 65% of the aggregate passage length. While forming, each first-order branch serves as a conduit for water fed by a rather discrete recharge source. Water converges into higher-order passages that become fewer and generally larger in the downstream direction. Closed loops are rare, except where water abandons its original route in favor of a new one and rejoins it, or a communicating passage, farther downstream. Branchwork caves are the subsurface hydrologic equivalent of dendritic river channels. In contrast, the following four are maze caves typified by many closed loops of synchronous origin.

Network caves are angular grids of intersecting fissures formed by the widening of nearly all major fractures within favorable areas of soluble rock (Figs. 1b and 3). They include 17% of the observed sample, both in number and in total length. Closed loops are common, and the straight, relatively high and narrow passages form a pattern like that of city streets. Some rudimentary networks consist of an angular array of dead-end fissures with few closed loops. Such fissures lack the individual recharge sources of branchwork caves.

Anastomotic caves consist of curvilinear tubes that intersect in a braided pattern with many closed loops (Figs. 1c and 4). They usually form a two-dimensional array along a single favorable parting or low-angle fracture. Rare

three-dimensional variants follow more than one geologic structure. Fracture-controlled segments may be present but do not dominate the pattern. Anastomotic mazes are usually superposed on branchworks and rarely constitute entire caves. Only 3% of the observed caves are predominantly anastomotic, but anastomotic passages account for 10% of the total sample length.

Spongework caves consist of interconnected solution cavities of varied size in a seemingly random three-dimensional pattern like pores in a sponge (Figs. 1d and 5). They represent 5% of the observed sample but less than 1% of the aggregate length. Most appear to have formed by coalescing of intergranular pores and minor interstices.

Ramiform (or ramifying) caves in plan view resemble ink blots or Rorschach patterns. Irregular rooms and galleries wander three-dimensionally with branches extending outward from the main areas of development (Fig. 1d). Passage interconnections are common, producing a continuous gradation with spongework and network caves. Abrupt variations in gradient and cross section are typical. Unlike those of a branchwork, ramiform passages are not convergent tributaries fed by different sources of surface recharge. Instead, many have served as sequential outlets for ground water. Ramiform caves constitute 4% of the observed sample and 8% of the aggregate length.

Single-passage caves are merely rudimentary forms of the types described above, although some reach large size. They include 14% of the observed caves but less than 1% of the aggregate length.

Passage Types

Many early theorists assumed that caves originate in the phreatic zone and are later invaded and enlarged by vadose water. The active parts of most caves, however, are well adjusted to the present pattern of recharge from the land surface, and so it is clear that few are preconditioned by an independent phreatic stage. The upstream reaches of a typical cave passage form in the vadose zone at the same time the downstream parts form in the phreatic zone. The question posed by early workers (for example, Davis, 1930; Swinnerton, 1932; Bretz, 1942) as to whether caves originate above, at, or below the water table is not pertinent.

The water table in a karst region is highly irregular and discontinuous because of great variations in the size and distribution of subsurface openings and in the amount of water they transmit. The water-table concept must be used with caution at the scale of individual cave



Figure 2. A junction of tubular stream passages in a typical branchwork cave (Binkley's Cave, Indiana).

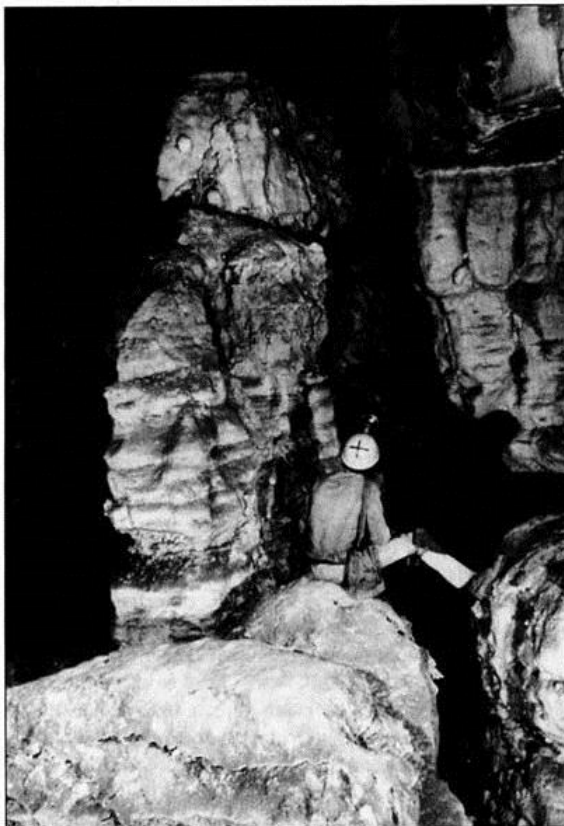


Figure 3. Intersecting fissures in a network cave (Wind Cave, South Dakota).

passages; yet it is nearly always possible to tell from passage morphology whether a particular reach of cave originated under vadose or phreatic conditions. Common passage types are shown in Figure 6 and are discussed in detail by Palmer (1984a), White (1988), and Ford and Williams (1989).

Figure 6 is a map and profile of a typical cave, a rudimentary branchwork with local anastomotic sections, which forms a continuous series of conduits linking surface recharge points to a single spring in the nearest entrenched valley. The cave was formed by underground diversion of a perched surface stream draining 3.5 km², which now flows into the cave entrance (A) only during wet seasons and floods. During low flow, it sinks several hundred meters upstream and enters the mapped area through a water-filled fissure at G. A tributary passage (C) originated as an earlier route for the main stream but is now fed only by seepage through soil. Trickles of infiltrating water enter at a few other points. Only a few passages remain perennially water filled. Flow through the cave varies from several hundred liters/sec to a maximum of several m³/sec. During high flow, the entire cave fills with water, with a 23-m head difference between entrance and spring.

Passages of vadose origin are formed by gravitational flow and trend continuously downward along the steepest available openings (Fig. 6, A-E). Most vadose passages are canyon-like with floors entrenched below the initial route by free-surface streams (B, C). They may be tubular where entrenchment is limited by resistant beds or insufficient time. Water descending vertically along a fracture or a cluster of intersecting fractures may form a shaft, a well-like void with nearly vertical walls (D). A typical vadose passage consists of inclined canyons or tubes interrupted in places by shafts.

Phreatic passages originate along routes of greatest hydraulic efficiency (least expenditure of head per unit discharge). Such a passage enlarges solutionally over its entire perimeter and usually acquires a rounded or lenticular cross section. Most are tubular passages (Fig. 6, F and X) and fissures (G), although some phreatic caves are irregular and room-like (Fig. 5). Floor sediment may impede downward dissolution. A passage along the water table may be water filled only during high flow and still meet the criteria for phreatic origin. Many have undulatory profiles containing one or more downward loops that extend below the water table, with only the high points of the loops reaching upward to the water table (Fig. 6, J; Ford, 1971). Early in the solutional history of a karst aquifer, the water table lies well above the fluvial base level; with only a small amount of enlargement,

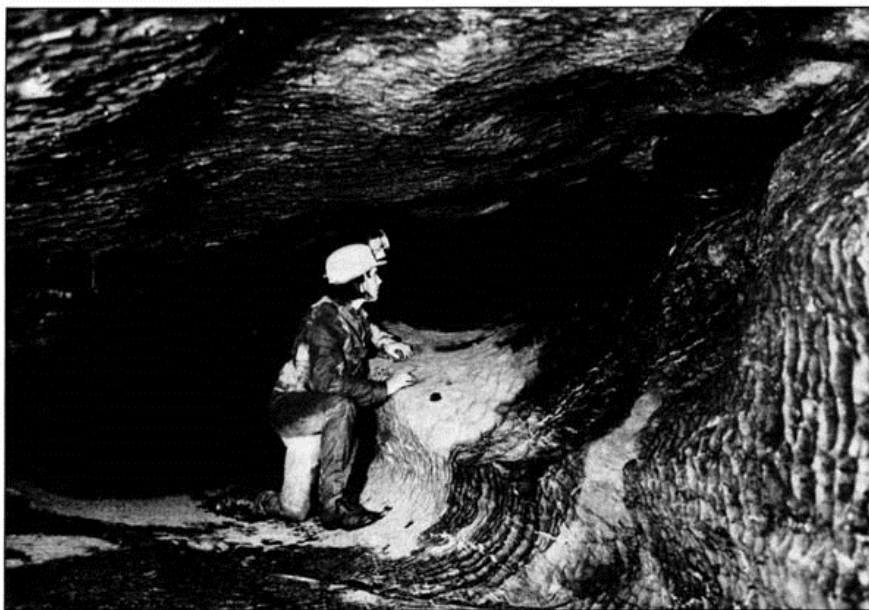


Figure 4. Junction of anastomotic passages formed along a dipping bedding-plane parting, Onesquethaw Cave, New York.

however, a phreatic passage transmits water so readily that the hydraulic gradient within it becomes very low. The low-gradient irregular profile downstream from F in Figure 6 is typical of a passage of phreatic origin.

With time, as the fluvial base level drops relative to the local strata, water in a phreatic passage acquires a free surface and may entrench

the floor, forming a keyhole-shaped cross section. More often, the water abandons the passage entirely in favor of a lower route. The original transition from vadose to phreatic conditions can be recognized, even in caves now totally dry, by a change in the downstream direction from steep downward-oriented passages (usually shafts and canyons) to undulatory tubes



Figure 5. Irregular rooms in Carlsbad Cavern, New Mexico, a cave of spongework and ramiform pattern.

or fissures of low overall gradient, as at point F in Figure 6.

Flood waters temporarily raise the water table in caves far above its normal level, modifying pre-existing passages, creating new ones, and blurring the distinction between vadose and phreatic cave development. Superposed on the main passages in the flood-prone cave in Figure 6 are upward-extending solutional fissures (Fig. 6, G) and complex anastomotic by-passes around constrictions (F, H). These features are rare in branchwork caves that have not been exposed to periodic flooding.

EPIGENIC AND HYPOGENIC CAVE ORIGIN

Epigenic caves are formed by the movement of water from overlying or immediately adjacent recharge surfaces to springs in nearby valleys. Of the caves in the observed sample (both in number and length), 90% are of this type. They include all cave patterns described above, although ramiform caves are poorly represented.

Significant dissolution of carbonate rocks requires acidic water. The most abundant epigenic acid is carbonic acid from CO_2 in the atmosphere and soil. Organic acids are usually far less important. Hypogenic caves are formed by acids of deep-seated origin, or epigenic acids rejuvenated by deep-seated processes. Such caves have no relation to recharge through the overlying surface. Most are of ramiform, network, or spongework pattern. The major hypogenic acids are hydrosulfuric acid (aqueous H_2S) and carbonic acid originating from redox reactions and igneous activity. H_2S and iron sulfides oxidize in moist air or oxygen-rich water to form sulfuric acid. Solutional aggressiveness can be renewed or enhanced by mixing of waters of contrasting chemistry (Bögli, 1964), particularly those differing in CO_2 or H_2S content or salinity. In this paper, except where otherwise stated, epigenic carbonic acid is considered the dominant solutional agent.

RATES OF LIMESTONE DISSOLUTION

To explain the variety of cave patterns, it is necessary to consider the relative rates of dissolution among the initial competing flow paths. The quantitative sections that follow are expansions of earlier work (Palmer, 1981, 1984a, 1984b, 1988). A solutional cave can form only where dissolution rates are sufficient to enlarge openings to appropriate size (for example, traversable by humans) before the rock is destroyed by surface processes. Denudation rates for carbonate rocks, estimated from dissolved

load in springs and rivers, are approximately 10–100 mm/1,000 yr and depend most strongly on amount of precipitation (Smith and Atkinson, 1976). Surface lowering accounts for about 50%–90% of this total (Ford and Williams, 1989). The remainder takes place below the soil/bedrock contact as cave and pore enlargement. Epigenic caves develop synchronously with the surrounding landscape, and so their lifespans rarely exceed a few million years. This is not necessarily true for hypogenic caves.

The Solutional Mass Balance

As a cave enlarges, bedrock dissolved from the walls must be carried away in solution by moving water. Within a given increment of passage length (dL) the mass balance for the rate of increase in cross-sectional area (dA/dt) is

$$\frac{dA}{dt} = \frac{31.56 Q}{\rho_r} \frac{dC}{dL} \quad \text{cm}^2/\text{yr} \quad (1)$$

where Q = discharge of water through the passage (cm^3/sec), dC/dL = increase in concentration of dissolved bedrock with distance (mg/L/cm), and ρ_r = rock density (maximum of 2.7 g/cm^3 for calcitic limestone). The coefficient 31.56 converts seconds to years, grams to milligrams, and liters to cm^3 .

Enlargement rate is examined here for the end members in the spectrum of passage shapes: tubes of circular cross section and planar fissures. The increase in area (dA) = $2\pi r dr$ in tubes and bdw in fissures, where r = tube radius, and w and b = narrow and long dimensions of the fissure cross section. The following equation applies to passage segments of finite length (L) and essentially constant cross section:

$$S = \frac{31.56 Q (C - C_0)}{p L \rho_r} \quad \text{cm/yr} \quad (2)$$

where S = rate of solutional wall retreat (dr/dt in tube, $dw/2dt$ in fissure), p = wetted perimeter

($2\pi r$ in tube, $2b$ in fissure), C = solute concentration, and $C_0 = C$ at the upstream end of the segment.

Discharge Rates in Caves

Discharge through a cave passage depends either on the amount of available recharge (catchment control) or on the hydraulic capacity of the passage (hydraulic control) (Palmer 1984a). In catchment control, which is far more common, discharge depends on the catchment area feeding the passage and the water surplus within that area. An example is a karst depression feeding a vadose passage. In hydraulic control, there is sufficient water to maintain closed-conduit flow throughout the passage. Excess water overflows via alternate routes. Ground water fed by an influent surface stream may initially be under hydraulic control, but when the conduits enlarge enough that their ca-

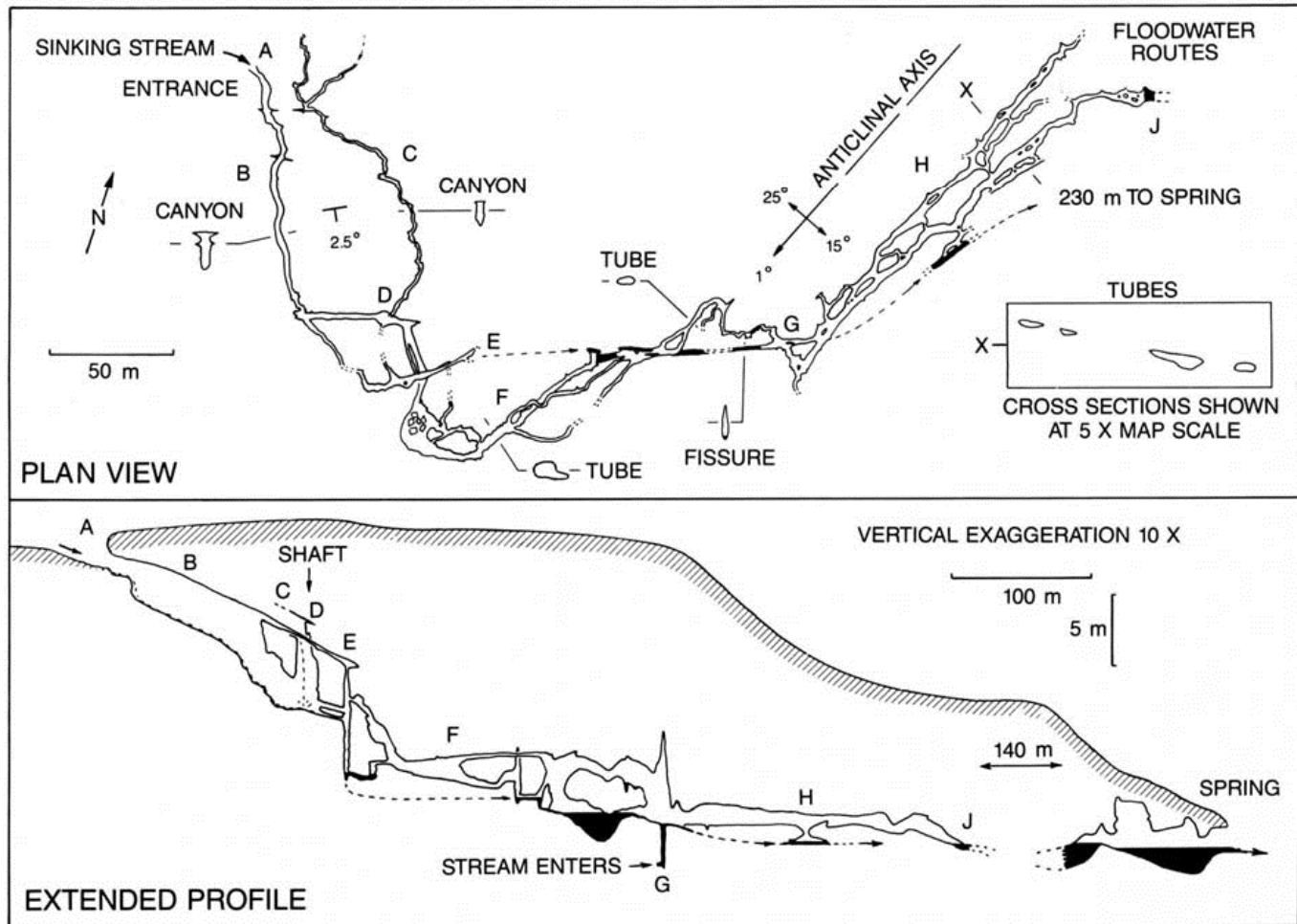


Figure 6. Map and profile of Onesquethaw Cave, New York, showing passages formed under vadose, phreatic, and flood-water conditions (from Palmer, 1972).

capacity exceeds the stream flow, the system changes to catchment control, and part or all of the water acquires a free surface.

Flow in pre-solutional openings is almost exclusively laminar. As dissolution proceeds, turbulent flow develops in those openings that enlarge to sufficient size ($w = \sim 1-20$ mm, depending on hydraulic gradient and temperature). Closed-conduit laminar flow is governed by the Hagen-Poiseuille equation:

$$Q = \frac{R^2 \gamma i A}{c \mu} \quad (3)$$

where R = hydraulic radius ($r/2$ in tubes, $w/2$ in fissures); $c = 2$ in tubes and 3 in fissures; γ and μ are the specific weight and dynamic viscosity of water; and i = hydraulic gradient expressed as a positive dimensionless number (head loss/flow length). Linear discharge, q ($= Q/b$ = velocity \times width), is a convenient term used in fissures of unspecified b dimension.

Turbulent flow in any closed conduit or open channel is expressed by the Darcy-Weisbach equation:

$$Q = A \sqrt{\frac{8 R g i}{f}} \quad (4)$$

where g = gravitational field strength and f = friction factor. In fully turbulent flow, $f = 0.03-0.1$ in a typical straight tube or fissure. Apparent friction factors, which include local head losses at bends and cross-sectional area changes, can be much higher (Lauritzen and others, 1985). Turbulent flow develops at a Reynolds Number (N_r) > 500 . $N_r = \rho v R / \mu$, where ρ and v = water density and velocity. In this paper, N_r is calculated using hydraulic radius, rather than pipe diameter, so that it applies to all conduit shapes.

Solutional Capacity of Ground Water

The saturation concentration (C_s) of dissolved calcite in water at various temperatures and P_{CO_2} was determined by iterative calculation of all relevant equilibria, including those for ion pairs, while observing electroneutrality, stoichiometric balance, and corrections for ion activity. Carbonate equilibrium constants were calculated with the empirical equations of Plummer and Busenberg (1982). Other equilibria here and elsewhere in this paper were determined from thermodynamic data of Wagman and others (1982). Results are shown in Figure 7. For example, in an open system at 10 °C with initial $P_{CO_2} = 0.02$ atm, dissolved calcite reaches equilibrium at C_s ($CaCO_3$ equivalent) = 273 mg/L, CO_2 concentration = 47 mg/L, and $pH = 7.12$. Total pressure of 1.0 atm is assumed; pressures up to 25 atm, equivalent to a depth of

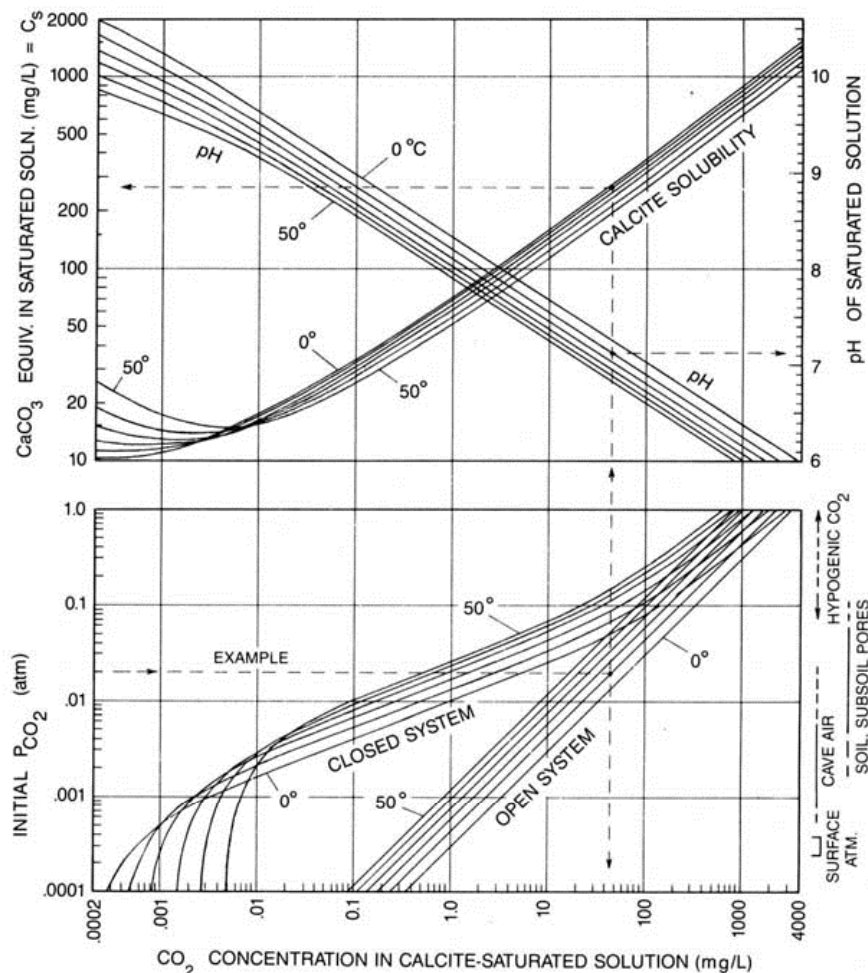


Figure 7. Saturation concentration of dissolved calcite (C_s) versus initial P_{CO_2} , equilibrium CO_2 , and equilibrium pH (modified from Palmer, 1984c).

~ 260 m below the water table, have little effect on the equilibria. These C_s values do not apply precisely to all limestone bedrock because of differences in composition from the pure calcite used in laboratory experiments.

Dissolution Kinetics

Dissolution rates in the CO_2 - H_2O - $CaCO_3$ system have been determined experimentally at pH values similar to those of natural ground water by Plummer and Wigley (1976), Plummer and others (1978), Sjöberg and Rickard (1984), and Buhmann and Dreybrodt (1985a, 1985b). Similar studies with dolomite have been made by Busenberg and Plummer (1982) and Herman and White (1985). These experiments show that at $pH > 4$, typical of nearly all karst ground water, the rate-limiting step is the reac-

tion at the bedrock-water interface rather than mass transfer within the water. Dissolution rate depends on the chemical undersaturation of the water, but only weakly on flow velocity or turbulence. Plummer and others (1978) expressed dissolution rate in terms of activities of dissolved species. More comprehensive models that include hydrodynamics are under development (Rosenfeld, 1986, based on Curl, 1968). In the present paper, to avoid dependence on a specific model and for convenience in geomorphic application, experimental data are fitted to this commonly used rate equation:

$$\frac{dC}{dt} = \frac{A' k}{V} (1 - C/C_s)^n \quad \text{mg/L-sec} \quad (5)$$

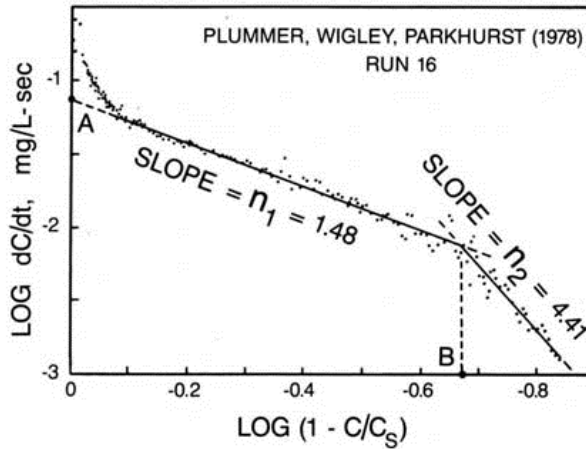
where A' = surface area of rock in contact with water (cm^2), V = water volume (cm^3), k = reaction coefficient (mg-cm/L-sec), and n = reaction

TABLE 1. VALUES OF k AND n IN EQUATIONS 5-7 FOR PURE AND IMPURE CALCITE

P_{CO_2} (atm)	n_1	5 °C			15 °C			25 °C		
		k_1		$(C/C_s)_T$	k_1		$(C/C_s)_T$	k_1		$(C/C_s)_T$
		Pure	Impure		Pure	Impure		Pure	Impure	
1.0	1.5	0.11	0.07	0.8	0.14	0.09	0.85	0.18	0.12	0.9
0.3	1.6	0.044	0.03	0.65	0.055	0.035	0.7	0.065	0.04	0.8
0.03	1.7	0.014	0.009	0.6	0.018	0.015	0.7	0.028	0.02	0.8
0.003	2.2	0.01	0.006	0.6	0.015	0.01	0.7	0.02	0.015	0.8

Note: all values $\pm 10\%$ – 20% , based on experimental data of Plummer and Wigley (1976) and Plummer and others (1978). See Figure 8 for method of calculation. $(C/C_s)_T$ = saturation ratio at the transition from low to high reaction order (n_1 to n_2); $n_2 = 4$; $k_2 = k_1 [1 - (C/C_s)_T]^{(n_1 - n_2)}$; units of k = mg-cm/L-sec.

Figure 8. Method used to determine the n and k values in Table 1, using experimental data by Plummer and Wigley (1976) and by Plummer and others (1978). A = $\log (A'k/V)$; B = $\log \{1 - (C/C_s)_T\}$; k_2 is found by solving equation 5 simultaneously for the two lines at $(C/C_s)_T$.



versus time in calcite dissolution experiments by Plummer and Wigley (1976) and Plummer and others (1978). C_s was calculated from the P_{CO_2} specified for the experiments, as in Figure 7, and Ca^{++} was found from the charge balance. Equilibrium was assumed for all dissolved species except calcite. $\log (dC/dt)$ was plotted against $\log (1 - C/C_s)$, and k and n were found by regression analysis (Fig. 8). This approach is similar to that of Plummer and Wigley (1976), except that the dimensionless term $(1 - C/C_s)$ is used instead of $(C_s - C)$ to avoid changes in units of k as n varies. An initial high-order rate shown by the experiments at $C/C_s < 0.1$ (Fig. 8) does not appear in measurements of limestone dissolution by Rauch and White (1977) and Howard and Howard (1967) and is excluded from Table 1. These earlier workers measured the Ca^{++} concentration, rather than pH. Ca^{++} concentrations determined from pH alone can be inaccurate at low C/C_s , because the slowness of CO_2 hydration prevents equilibrium of aqueous species during rapid dissolution. Unless otherwise specified, k values used in this paper are those of impure calcite, which approximates that of natural limestone (see Figs. 9 and 10).

At any point in a growing conduit, the rate of solutional wall retreat (S) is found by combining equations 1 and 5:

$$S = \frac{31.56 k (1 - C/C_s)^n}{\rho_r} \text{ cm/yr.} \quad (6)$$

Equation 6 is valid for any kind of water flow in contact with limestone at $pH > 4$. If equation 5 is integrated and combined with the relationships $V/t = Q$ and $A' = 2\pi rL$ in a tube and $2bL$ in a fissure, the saturation ratio at the downstream end of a passage segment of length L (all other terms held constant) is

$$C/C_s = 1 -$$

$$\left[\frac{p L k (n-1)}{Q C_s} + (1 - C_0/C_s)^{(1-n)} \right]^{1/(1-n)} \quad (7)$$

where $n \neq 1$.

Laboratory and Field Measurements of Limestone Dissolution

In their experiments, Plummer and Wigley (1976) and Plummer and others (1978) used crushed Iceland spar suspended in turbulent water. Values of n and k in Table 1 are derived from this work, and their validity in typical karst ground water must be shown before equations 5-7 can be applied to cave origin.

Rates estimated by equation 6 compare well with those measured in artificial tubes in limestone and dolomite by Rauch and White (1977)

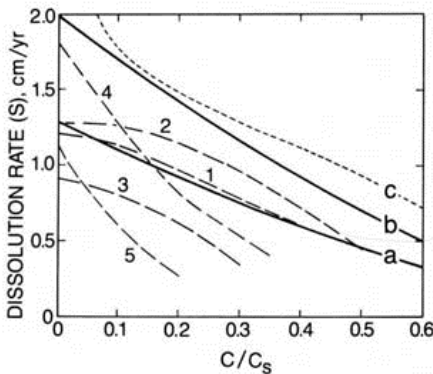


Figure 9. Dissolution rates of limestone and dolomite, averaged from laboratory measurements of 17 experiments by Rauch and White (1977) at 23 °C and $P_{CO_2} = 1$ atm: 1 = pure limestone, 2 = limestone with silty wisps, 3 = limestone with detrital impurities, 4 = dolomitic limestone, 5 = dolomite with detrital impurities. Rates estimated by equation 6 are shown for comparison, using k for impure calcite (a), and for pure calcite (b). Line c is the dissolution rate for pure calcite according to the equation of Plummer and others (1978).

order. Values of n and k vary with saturation ratio (C/C_s), temperature, and P_{CO_2} . Ideally, C should be measured at the solid surface, but mass transfer, even in standing water, is rapid enough that C is nearly constant throughout the cross section.

Table 1 lists values of k and n determined by this writer from free-drift measurements of pH

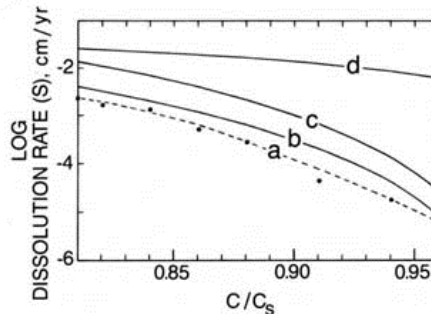


Figure 10. Dissolution rates of calcite at high C/C_s for $P_{CO_2} = 0.003$ atm and $T = 25$ °C: (a) measured by Morse (1978), and estimated by equation 6 using k for impure calcite (b), and for pure calcite (c). Line (d) is the rate estimated by the equation of Plummer and others (1978).

at 23 °C and $N_r = 460$ (Fig. 9). An open system was simulated by recirculation of water through a CO_2 chamber. Their study showed that dissolution rate decreases with dolomite content, crystal size, and percent insoluble material (except where it forms minor silty wisps). The dissolution rate of oceanic carbonate sediment at high C/C_s was measured in artificial sea water by Morse (1978). His data (Fig. 10) agree well with equation 6, which gives evidence that ionic strength has little influence on limestone dissolution rate.

Laboratory measurements of dissolution rate in laminar flow through artificial fractures in limestone were made at low C/C_s by Howard and Howard (1967). Their experiments approached apparent equilibrium at a concentration only 90% of that shown in Figure 7, which suggests that the slowing of dissolution rate shown in Figure 8 also occurs in laminar flow. Measurements of calcite dissolution in thin water films by Buhmann and Dreybrodt (1985b) agree well with those of Howard and Howard. Rates are about half those of equation 6, but the functional relationships described here are not affected.

Field measurements combining enlargement rate with mean-annual water chemistry are almost non-existent. Limestone retreat has been measured with mounted indicator dials in cave streams (High, 1970; Coward, 1975). Direct comparison with equation 6 is difficult without continuous chemical records, but their measurements of 0.04–0.08 cm/yr are compatible with the predicted rates.

EVOLUTION OF A SINGLE CAVE PASSAGE

It is necessary to examine the evolution of a single conduit before the pattern of a complex cave can be understood. Consider a system of presolutional fractures and partings deep beneath the surface. Hydraulic gradients, discharge, and dissolution rates are at first negligible, but they increase as fluvial entrenchment exposes the soluble rock. For now, the complexities of recharge are ignored and attention is focused only on a series of interconnected openings that eventually enlarge into a single cave passage.

For convenience, the conduit is considered entirely water filled during its early stages of development. The equations for dissolution rate derived earlier are valid whether the system is open or closed with respect to a CO_2 gas phase. Perfectly closed systems are rare in nature, but water-filled conduits provide a fair approximation. At the upper end of such a conduit, aqueous CO_2 is in equilibrium with the gas phase

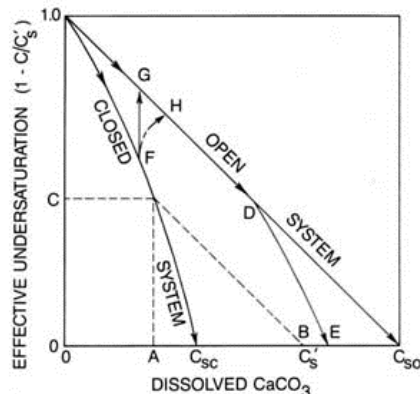


Figure 11. Chemical evolution of cave water under open and closed conditions. The effective saturation concentration of dissolved calcite (C_s') drops as dissolution proceeds under closed conditions, and so rates are less than in open systems of similar initial conditions. C_{so} and C_{sc} = saturation concentrations in purely open and purely closed systems, respectively. At concentration A, $C_s' = B$ and the effective undersaturation is C. Water flowing from an open to a closed system evolves along a line similar to D–E. From a closed to an open system, it first follows a line similar to F–H, and then the open-system line. Line F–G is the ideal, never achieved, in which the uptake of CO_2 in the open system is instantaneous.

upstream from it. The dissolution rate at the beginning of the closed section is equal to that in a comparable open system, but as C increases downstream, the dissolved CO_2 content decreases in the closed conduit, causing an apparent decrease in C_s . The effective value (C_s') decreases toward the C_s for the closed system (Fig. 11). Dissolution is slower than in an open system, where C_s remains constant. The decrease in C_s' is not quite linear with increasing C , but less than 10% error is incurred by assuming that it is. C_s values for calcite in open and closed systems are shown in Figure 7.

Equations 2 and 7 allow the growth rate of any water-filled passage to be calculated. Results for $C_0 = 0$ and initial $P_{\text{CO}_2} = 0.01$ atm at 10 °C are shown in Figure 12. The curves for i/L (hydraulic gradient/length, cm^{-1}) are valid only for laminar flow (eq. 3). In a closed conduit, n and k change as C_s' diminishes with distance of flow. Mean dissolution rates in Figure 12 were obtained by finite-difference calculations in which each presolutional fracture was divided into 100 length increments and C_s' was adjusted linearly between 212 and 55.6 mg/L (initial and final

saturation values as dissolution proceeds in a closed system). The n and k values were varied accordingly by interpolation from Table 1. The largest feasible bedrock density (2.7 g/cm^3) was assumed. The basic shapes of the graphs in Figure 12 are independent of the n and k values used to compute them. Although this figure is intended mainly for conceptual purposes, the following example clarifies the relationships: if $Q = 0.01 \text{ cm}^3/\text{sec}$ through a 10,000-cm-long tube of radius 0.1 cm, $Q/L = 10^{-6} \text{ cm}^2/\text{sec}$. The corresponding $i/L = 10^{-6.47}$, and $i = 0.0034$. If $C_0 = 0$, the mean dissolution rate in the tube will be $\sim 10^{-2.8} \text{ cm/yr}$. Figure 12 shows a range of enlargement rates from infinitesimal to surprisingly rapid. Development of traversable caves at growth rates less than 10^{-6} cm/yr is not feasible, except in unusually stable geologic settings.

Several observations can be made from Figure 12 that apply to cave origin by the CO_2 reaction: (1) The rate of solutional wall retreat increases with discharge but reaches a maximum, at which a further increase in discharge has no effect (unless accompanied by variations in P_{CO_2} or temperature). In typical ground water, the maximum rate of wall retreat averages about 0.01–0.1 cm/yr, achieved when Q/rL or q/L exceeds 0.001 cm/sec. (2) At low discharge, typical of passages in their earliest stages, there is great variation in mean enlargement rate among competing flow routes. (3) Incipient passages can increase their growth rate only by acquiring more discharge. (4) Where many alternate flow routes have steep gradients, short lengths, and rather uniform chemistry, all will enlarge at nearly equal rates, regardless of size.

The origin of a limestone cave hangs by a delicate thread. For it to reach traversable size in a feasible time, dissolution must be rapid; yet too high a rate is detrimental to its early development. In a narrow crack, rapid dissolution would cause near-saturation after only a few centimeters of flow, and enlargement downstream would be negligible. Only slow, uniform dissolution can initiate long passages. This paradox is reconciled by the abrupt slowing of dissolution while the water is still far from saturation (Fig. 8). This transition, first observed by Berner and Morse (1974), is expressed by the increase in reaction order (n). Because $(1 - C/C_s)$ is less than 1.0, S decreases as n increases. Palmer (1984b) demonstrated that without this change, caves, and therefore major karst features, could form only where gradients and initial widths are exceptionally large (for example, along escarpments). Instead, dissolution at high n allows slow, nearly uniform enlargement of initial openings over long distances, and when water is eventually able to penetrate the entire length of this primitive route at low C/C_s , rapid

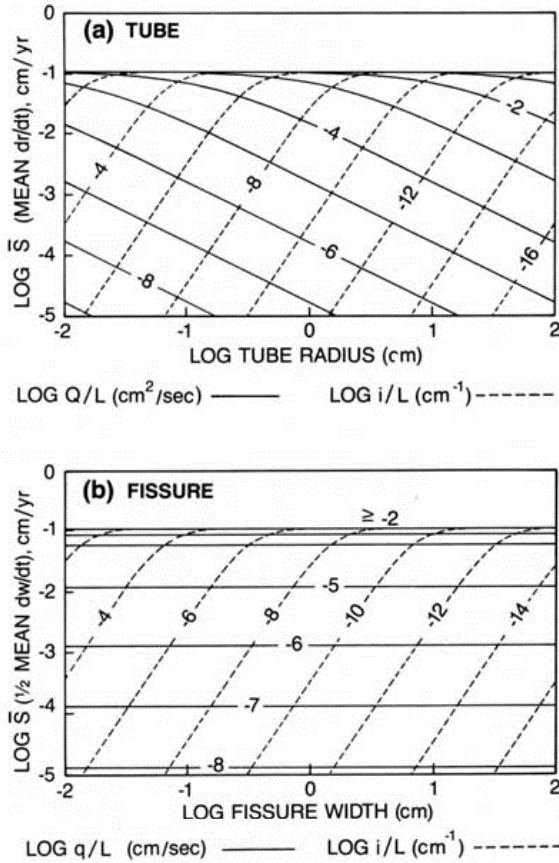


Figure 12. Mean rate of solutional wall retreat (S) versus discharge (Q), flow length (L), and passage radius (r) in a tube, and versus passage width (w) in a planar fissure under typical ground-water conditions (initial $P_{CO_2} = 0.01$ atm, $T = 10^\circ\text{C}$, closed system).

stages. To obtain this information, equations 2 and 7 were used iteratively to calculate the growth history of idealized fissures of various length (L) and initial width (w_0) at fixed hydraulic gradients (i). Each was divided into 100 length increments and its solutional history into at least 500 time steps. To avoid sharp discontinuities in enlargement rate, the length segments were shortened in the upstream direction in inverse proportion to the initial dissolution rate. The appropriate flow equation (eq. 3 or 4) was selected on the basis of Reynolds Number, and Q was calculated from a weighted mean of all segment widths. C_s , n , and k were adjusted as C increased, as in Figure 11. The time (t_{max}) required for the rate of fissure enlargement at the downstream end to reach its maximum is shown in Figure 13. After the transition from high to low reaction order takes place, the maximum dissolution rate is achieved in less than 0.1% of t_{max} . Because i and L have equal but opposite effects, they are combined as a single term. The calculations produce the family of lines

$$t_{max} = \alpha w_0^{-3.12} (i/L)^{-1.37} (P_{CO_2}^0)^{-1.0} \text{ yr} \quad (8)$$

where $P_{CO_2}^0$ is the CO_2 partial pressure at the upstream end and α is a coefficient controlled by temperature and type of system. At 10°C , $\alpha = 5 \times 10^{-12}$ for closed systems and 1×10^{-12} for open systems. Deviations from these lines occur only at $t_{max} < 100$ yr or when the time or length increments are inappropriately large. The t_{max} is also influenced by lithology, mixing, chemical reactions within the water, dissolution-inhibiting ions (for example, phosphate), and microbial CO_2 production. Figure 13 was determined with $n_2 = 4$. Although varying n_2 between 3 and 6 causes t_{max} to vary as much as 50%, there is no change in functional relationships, showing that early growth rates are only poorly dependent on kinetics. Typical i/L values in karst ground water are 10^{-3} to 10^{-7} cm^{-1} , rising to more than 10^{-2} during floods in caves fed by sinking streams. Field observations in Hungary suggest 0.001 cm as the minimum w_0 for cave origin (Böcker, 1969), a value compatible with Figure 13.

Comparison of equation 8 with equation 3 and Figure 7 shows that t_{max} is proportional to $(Lb/Q_0 P_{CO_2}^0) \sqrt{L/i}$, where Q_0 = initial discharge. Most early cave enlargement is at $C/C_s > 0.9$, and so C_0 has little effect on t_{max} .

The early growth history of an idealized fissure is shown in Figure 14. Two phases of cave development are evident: (1) an initial phase in which the enlargement rate is proportional to discharge but is nearly independent of kinetics and (2) a mature phase in which the cave has reached a maximum enlargement rate depend-

dissolution enlarges the openings to cave size. The effect is analogous to drilling a pilot hole for a nail. White (1977b) showed that at typical ground-water gradients the change from slow (high-order) to rapid (low-order) kinetics in a growing conduit coincides approximately with the laminar-turbulent transition and with the

onset of sediment transport. This combined step is the most significant threshold in the evolution of a cave.

The time required for a conduit to reach maximum growth rate cannot easily be determined from the graphs because of the large variation in dissolution rate over its length during the early

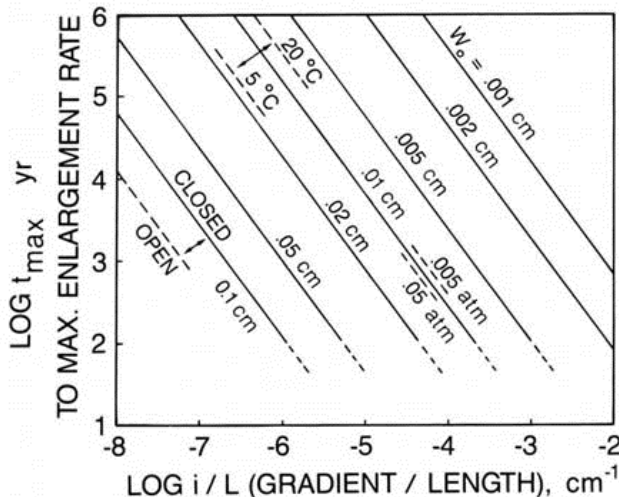


Figure 13. Time (t_{max}) required for ground water in a planar fissure to achieve the maximum rate of solutional wall retreat over its entire length, as a function of hydraulic gradient (i), flow length (L), and initial fissure width (w_0). The dashed lines show a decrease in t_{max} with P_{CO_2} and open system, and an increase with temperature.

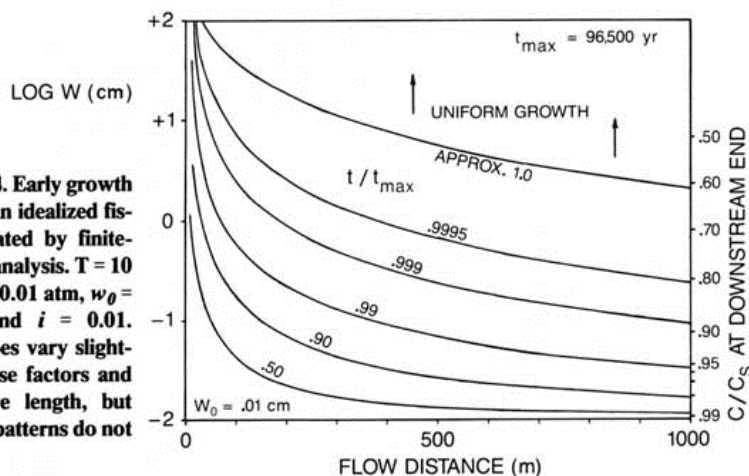


Figure 14. Early growth history of an idealized fissure simulated by finite-difference analysis. $T = 10^\circ\text{C}$, $P_{\text{CO}_2}^0 = 0.01 \text{ atm}$, $w_0 = .01 \text{ cm}$, and $i = 0.01$. Curve shapes vary slightly with these factors and with fissure length, but their basic patterns do not change.

ent on kinetics but almost independent of discharge. A typical cave passage probably spends more than half of its solutional history at very slow enlargement rates near saturation. The transition from (1) to (2) takes place over a relatively short time span.

Until the fissure has nearly reached the maximum dissolution rate over its entire length, almost all enlargement takes place in the upstream 10%. At t_{max} the width varies only about 0.5–1.0 m over the downstream 90% of the passage length. This taper is quickly obscured by the rather uniform growth from then on. Most cave passages do not narrow measurably in the downstream direction. The entrance area of a conduit develops a wide funnel shape that is more aptly considered part of the karst surface rather than of the cave. In soil-mantled karst, the wide upstream section remains filled with soil until the entire conduit enlarges enough that unconsolidated material can be removed by turbulent cave streams as it subsides from above. The upstream parts of most passages develop open-channel flow early, locally diminishing the contact with bedrock and the rate of increase in cross-sectional area.

The maximum enlargement rate can be calculated from equation 6, with C_0 substituted for C . It must be considered a weighted mean value that integrates seasonal variations. Seasonal fluctuations in hydraulics and chemistry are short lived compared with the time scale for cave development, and use of annual means is justified. Abrasion by stream-borne sediment can drive the rate higher than calculated by the equations (Newson, 1971). Sedimentary deposits, however, may shield the limestone from dissolution and limit passage growth. After a passage reaches the maximum annual enlargement rate, its size depends mainly on the length of time it

contains flowing water. Discharge and water velocity are of secondary importance, although after the water acquires a free surface, the wall area exposed to dissolution varies with flow conditions. Enlargement rates generally decrease when the cave becomes partly air filled and receives low- CO_2 air from the surface. If water enters a cave after passing through high- P_{CO_2} soil, degassing in the cave air reduces C_s . Water entering at or near saturation will deposit travertine. Some cave streams are supersaturated during all but the wettest periods, when overland flow dilutes the water from diffuse inputs. The net result is solutional stagnation throughout most of the year, with growth bursts during floods. In contrast, nearly all cave streams fed by runoff from noncarbonate rocks are undersaturated year round and enlarge at rates similar to those in Figure 12. The major growth of a passage ends when its water diverts to lower routes, but periodic flooding may allow further intermittent growth.

Dreybrodt (1988) independently computed the enlargement history of fissures in a manner similar to that used here (also see Palmer, 1984b, 1988). Assuming fixed first-order and fourth-order kinetics, he obtained sharp breaks in fissure width that differ from the smooth curves of Figure 14, but his t_{max} values are compatible with those shown here for open systems.

Figure 13 shows that under favorable conditions a cave requires a minimum of ~10,000 yr for its initial phase. Several thousand years more are required for it to reach traversable size (eq. 6; Fig. 12). These rates have been verified by radiometric dating of travertine in Bahamian caves by Mylroie and Carew (1987). Rates in typical ground water are probably slower by an order of magnitude. Passages in Mammoth Cave, Kentucky, have been dated by geomorphic relation-

ships (Miotke and Palmer, 1972), radiometric dating of travertine (Hess and Harmon, 1981), and paleomagnetism of sediments (Schmidt, 1982). In the past 730,000 yr since the last magnetic reversal, at least three separate passage levels have formed with diameters up to 10 m.

The conditions assumed in constructing Figures 12–14 are far simpler than those of natural systems. The hydraulic gradient (i), C_0 , and C_s vary with time in a real conduit (see Smart, 1988, on the influence of hydrologic variation on karst evolution). The initial fissure width is not constant over its length. The distribution of flow among interconnected paths changes as the openings undergo differential growth. Few ground-water systems are truly closed. Carbon dioxide generated by oxidation of organic material may augment dissolution rates deep within the conduit (Bray, 1972; Atkinson, 1977; Wood and Petraitis, 1984). In many places, CO_2 is carried into the system by infiltrating water, boosting C_s (Thraill and Robl, 1981). The resulting systems fall between the extremes of purely open or closed.

CONTROL OF CAVE PATTERNS BY GROUND-WATER RECHARGE

Combining the experimental rate data and analytical interpretations of cave growth with field observations makes it possible to answer two of the most fundamental questions about cave origin. Why do only a few of the myriad initial openings in limestone enlarge into caves? What determines the basic cave patterns?

Localization of Caves within a Carbonate Aquifer

Caves form by the selective enlargement of only a few of the many presolutional openings in the host rock. Even maze caves occupy small areas surrounded by relatively noncavernous rock. Most early cave enlargement is performed by small amounts of water traveling long distances through narrow openings, and so cave development begins low on the graphs in Figure 12. Only those routes that gain recharge (usually at the expense of their neighbors) grow fast enough to form true caves. All others languish with low and generally diminishing dissolution rates.

The most favorable flow paths for cave development are those with the smallest t_{max} (Fig. 13). As t_{max} is proportional to $(Lb/Q_0 P_{\text{CO}_2}^0) \sqrt{L/i}$, the shortest routes of greatest discharge and CO_2 content are selected. P_{CO_2} usually does not differ greatly among neighboring flow paths, but Q varies enormously. Fissure width is by far the most important variable in determining how

the available flow is distributed (eq. 3). In forming a cave, phreatic water can sacrifice a great deal of path directness in favor of a route with only a slightly greater effective width. This accounts for such roundabout passages as those in Figure 1c.

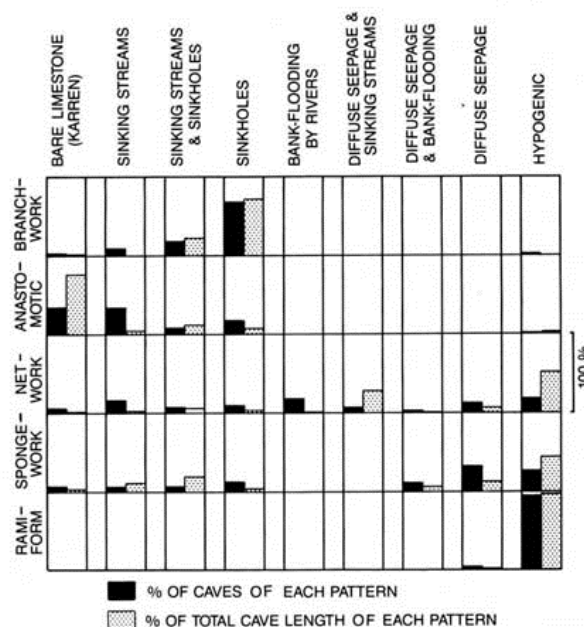
Cave origin is enhanced where surface runoff is concentrated into small areas of infiltration. Karst depressions serve this function but are secondary features that form only after cave development is underway. Ideal sites for initial cave development include perched stream valleys, glacial cirques, and contacts between insoluble and soluble rocks. The importance of favorable topography to cave origin is illustrated by the distribution of caves in the observed sample: 44% (67% by length) are now (or originally were) fed by valleys or sinking streams, and 18% (10% by length) are located at contacts between soluble and insoluble rock. Of the remaining, 70% of the length consists of hypogenic caves, such as Carlsbad Cavern (Figs. 1d and 5), which originated independently of surface recharge, and the rest are mainly relict fragments out of adjustment with their present setting.

Branchwork versus Maze Patterns

A large phreatic passage transmits water so efficiently that its head, despite large flow, is less than in surrounding openings. Water in adjacent openings converges toward large passages, producing a branchwork pattern. But if hydraulic gradients are steep and the flow paths short, dissolution quickly reaches a maximum rate (near the tops of the graphs in Fig. 12) along many alternate paths. Growth in all but the smallest openings is rather uniform, regardless of size, producing a maze cave. The same effect is achieved if each fissure in an array receives rather uniform recharge (Fig. 12b).

The nature of ground-water recharge is the most important factor in determining whether a cave will be a branchwork or a maze. Although influenced in turn by topography, lithology, soil type, and climate, ground-water recharge is the focal point through which all these diverse factors exert their control on cave patterns. Figure 15 shows the relationship between recharge and pattern for the caves in the observed sample. Branchwork caves are associated with discrete small-catchment sources (for example, sinkholes) typical of a karst surface. Maze caves are formed by either (1) surface runoff that enters the soluble rock either as sinking streams or as bank storage along entrenched rivers during floods, producing hydraulic gradients steep enough to achieve uniform passage enlargement along many alternate flow routes; (2) diffuse recharge through an overlying or underlying per-

Figure 15. Relationship between cave pattern and type of recharge into the carbonate aquifer for the caves in the observed sample. Total number of caves = 427; total length of caves = 2,315 km.



meable and usually insoluble rock, which contributes nearly uniform amounts of flow to each major fracture in the limestone; or (3) rejuvenated aggressiveness of ground water in many interconnected openings by mixing of waters of different chemistry, or by cooling of thermal water. Anastomotic mazes are produced only by sources that fluctuate greatly in discharge. Network and spongework caves form under a broad range of settings, including floodwater, diffuse recharge, and hypogenic conditions. Ramiform caves are almost all hypogenic. The following sections examine the origin of each cave type.

ORIGIN OF BRANCHWORK CAVES

Branchwork caves exceed in number and aggregate length all other caves combined, and so it is not surprising that they are formed by the most common type of karst recharge. Aggressive water concentrates in and beneath karst depressions and penetrates the aquifer at discrete points. Branchwork caves are formed by the convergence of stream passages, both open channels and closed conduits, mainly tubes, canyons, and shafts. Small depressions in bare, highly fractured rock can have a spatial frequency greater than 1,000/km². A single large depression may drain many square kilometers. Each point source has the potential to form a first-order tributary of a branchwork cave. Low-order passages join to form those of higher order and usually larger size. The outlet is commonly a single spring, although overflow springs may

occur where the main spring has been partly blocked. Large rooms form only at passage intersections, or where extensive collapse material has been removed in solution and as detritus by cave streams.

Blue Spring Cave, in the Mississippian Salem Limestone of Indiana, is a well-documented example of a branchwork cave (Fig. 16). More than 50 tributary passages join to form a single large stream passage draining to a spring on the entrenched East Fork of White River. As the river deepened its channel, many of the passages were abandoned by their flow in favor of lower routes. Abandoned passages, identified on the map by dashed lines, carry water only during floods. The maze sections shown in the insets were superposed on the branchwork pattern by flood-water activity.

Evolution of Karst Depressions and the Epikarstic Zone

The large amount of ground-water circulation required to form a branchwork cave is usually triggered by the entrenchment of major surface rivers. Small influent tributary streams lose water to the subsurface, forming the earliest depressions, whereas entrenched rivers serve as ground-water outlets. In the earliest phase of cave development, solutional aggressiveness is consumed mainly at the bedrock surface and in the first few meters of flow. Dissolution at depth is extremely slow.

Karst depressions form concurrently with caves. As a passage enlarges, increasing amounts

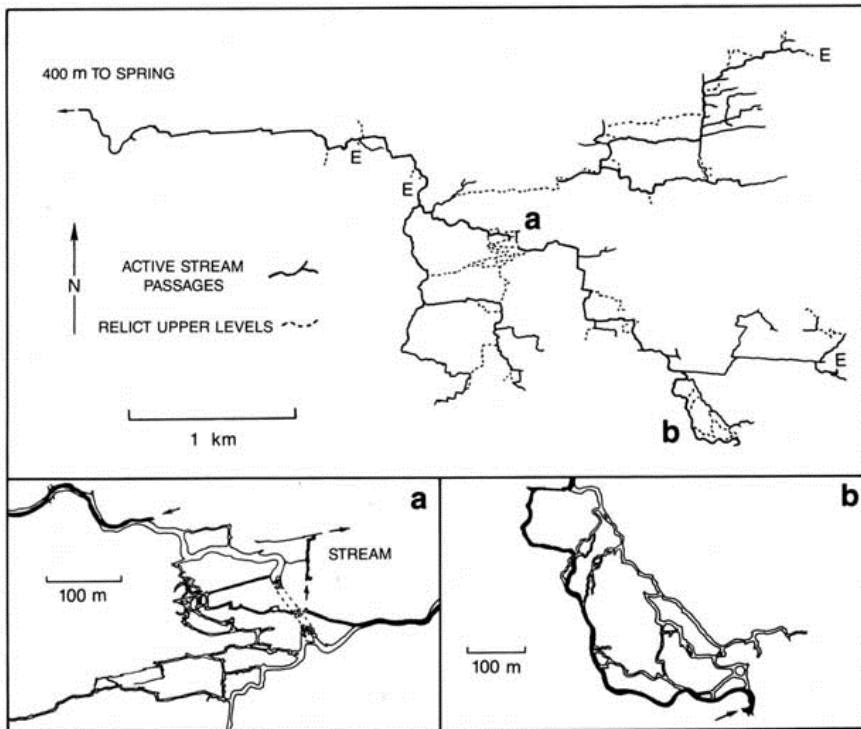


Figure 16. Map of Blue Spring Cave, Indiana, in prominently jointed Salem Limestone (Mississippian). The enlargements show a network maze bypassing a collapse in the main passage (a), and an anastomotic maze in an area of interbedded chert (b). Map from Palmer (1975).

of detrital material are removed from the feeder sinkholes by subsurface flow, enlarging them. As sinkhole catchments grow, greater amounts of water feed the major drain passage in a self-accelerating manner, robbing nearby openings of much of their flow (Fig. 17). Dissolution, subsidence, and collapse all contribute to the origin of depressions. Some have open holes at the bottom that feed runoff directly into underlying caves, but most are floored with regolith.

Recharge through sinkholes is more complex than it appears from the surface. Typically the upper few meters of limestone contain a myriad of solutionally widened fissures, which form the epikarstic (subcutaneous) zone (Williams, 1985). Most are soil filled. These openings result from epigenic dissolution at its most aggressive. Many competing flow paths enlarge at similar rates near the tops of the graphs in Figure 12. The fissures narrow rapidly downward, and therefore during wet periods, water moves through them with a large lateral component and empties into the relatively few openings that penetrate to greater depth as caves. In this way, dispersed recharge from a karst surface is focused subcutaneously into essentially point sources.

Development of Convergent Passages

Gravitational vadose water consists of discrete streams that have no hydraulic continuity with one another. Each passage of vadose origin follows an independent route with no inherent tendency to converge with its neighbors. Vadose canyons can extend parallel to one another for great distances without joining (Fig. 6, B and C). They are, however, commonly forced to converge by geologic structures such as intersecting joints or by synclines and basins in perching horizons. In passages of exclusively vadose origin, the branchwork pattern, if any, is inherent in the earliest flow.

Phreatic passages create zones of low head that attract phreatic water from surrounding openings. Much convergence is present even in presolutional openings, owing to differences in hydraulic efficiency, and the branching pattern of the resulting passages is simply inherited. Other branches develop by readjustment of flow paths as the head distribution changes with time. This evolution is shown schematically in Figure 18. Two adjacent flow routes in a presolutional fissure system are connected by route C. If route A is hydraulically more efficient than route B, h_1

will generally be less than h_2 , although the reverse may be true during the onset of floods. Some water will leak through C, depending on its length and effective width, and on the magnitude and sign of $(h_2 - h_1)$. If C grows more rapidly than B, the resulting passages will converge. Head differences between flow paths are greatest in the upstream reaches far from springs, and confluence is favored in those areas, unless structural variations dictate otherwise.

Whether convergence is achieved depends on which route, C or B, has the smaller t_{max} . Both are fed by the same source, and therefore the initial chemistry and temperature are identical. The smaller t_{max} will be in the route having the greater value of $w_0^{3.12} (i/L)^{1.37}$ (eq. 8). If t_{max} is less in C, convergence of the resulting passages is virtually certain. When either B or C approaches its maximum dissolution rate, it will grow rapidly, while the other remains no more than a few millimeters in average width, and usually far less. The less favorable route might also enlarge to cave size in time, but its t_{max} is lengthened so much by the diminishing hydraulic gradients that it is unlikely to do so before being abandoned entirely by a drop in water table.

Linkages of this kind at various times throughout the aquifer help to determine the layout of branchwork caves. Ewers (1982) has simulated this process with salt, gypsum, and plaster models. He injected aggressive water under pressure into the planar contact between the soluble material and a transparent pressurized bladder, through which the developing solution conduits were observed. In the models, the steep hydraulic gradient, high aggressiveness, and initial anastomotic patterns simulate flood-water conditions (described below) rather than pure branchwork cave development. Although quantitative results cannot be extrapolated to the field because of differences in solution kinetics, this work illustrates how a single large conduit can draw water from surrounding immature ones to form a branchwork.

The models showed a cascading effect, in which the linkage of each tributary to a pre-existing passage caused a sudden drop in hydraulic gradient within the tributary and a rearrangement of the surrounding potential field. In nature, this effect is less pronounced, because most passages become linked while still in their initial stages of development, and because gradients are much smaller and more uniform than in the models.

Influence of Physical Setting on Branchwork Caves

The broad variety of geologic settings and climates in which branchwork caves occur sup-

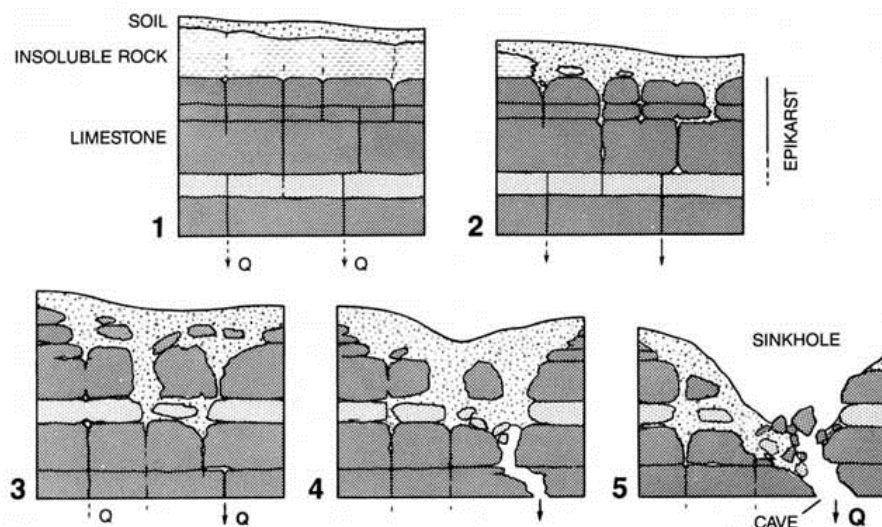


Figure 17. Evolution of the epikarst and a typical solutional sinkhole. The lightly shaded bed is a visual aid in comparing stages.

ports the premise that the branching pattern depends only on the presence of depression recharge. Other variables merely control the shape and orientation of individual passages. A few examples are described below.

Prominent joints are often cited as the cause of network caves. On the contrary, some of the most prominently jointed rocks, such as the Salem Limestone of Indiana, contain branchwork caves almost exclusively, but very few networks, most of which are superposed on branchwork caves. Joints impose an angular passage pattern on the branchwork layout. Parts of Blue Spring Cave (Fig. 16) follow single joints for more than 200 m with passage widths of less than 3 m. In contrast, prominently bedded rocks contain curvilinear passages.

Carbonate rocks of high primary porosity contain mainly spongework caves, but crude branchworks form if there is sufficient flow. For example, the Rio Encantado Cave, Puerto Rico, in porous Tertiary limestone, consists almost entirely of a single stream passage more than 10 km long. Water enters through numerous tiny openings, but only a few short tributaries are traversable.

A partial cover of impermeable rocks limits the surface area available for direct recharge to underlying caves. Branchworks are still favored, but they have few tributaries. An example is McFail's Cave, New York, which is capped in all but its northern end by impermeable rocks and glacial till (Fig. 19a). Its mapped length of 10 km consists essentially of two passages: a down-dip canyon and a tube oriented nearly parallel to the strike.

Stratal dip exerts a strong influence on passage trend. Most vadose passages, because they are formed by gravitational water, are dip oriented. Phreatic passages follow the most efficient paths, which are usually at or just below the water table because of diminishing fissure width and frequency with depth (compare with Ford, 1971). In well-bedded rocks, most are nearly parallel to the strike, draining in the direction of the nearest entrenched valley. Specific passage orientations differ, but the over-all branchwork pattern is present regardless of dip direction or angle. Figure 1a shows a cave in rocks dipping gently to the northeast at less than 1° . Vadose passages converge northeastward

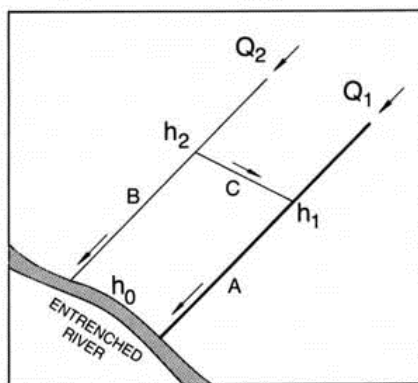


Figure 18. Development of a branchwork under phreatic conditions. Convergent passages develop only if C grows faster than B. See text for details.

toward southeastward-oriented passages of phreatic origin. In steeply dipping strata (Figs. 6 and 19b), vadose passages descend abruptly in short direct paths to phreatic passages, most of which are highly linear along the strike, unless prominent fractures impose other trends.

Branchwork caves are well adjusted to the geomorphic history of the valleys to which they drain. During fluvial entrenchment, water in base-level cave streams tends to divert to successively lower levels. Where many passages have been abandoned by their original flow, the branchwork pattern of active passages is obscured on cave maps (Figs. 16 and 19b). In a multi-level cave, the largest passages are those that have remained active for the longest time. They generally correlate with periods of nearly static base level (for examples, see Powell, 1970; and Palmer, 1987).

Climate affects cave patterns only indirectly, by controlling the rate and character of recharge. In arid climates, branchwork caves are uncommon because of limited surface recharge. Hypogenic acids, if present, are likely to dominate cave origin. Tropical caves formed at high P_{CO_2} may enlarge faster than caves in other climates, but their morphology is not significantly different. At high temperatures, the rapid dissolution rate actually increases the time required for a cave passage to form (Fig. 13), because dissolution is concentrated at the upstream ends of passages. The opposite is true in alpine and arctic karst. In alpine karst, the typical cave is a steeply descending shaft-and-canyon series with many small vadose inlets fed by bare, seasonally snow-covered bedrock surfaces. Their branching pattern, although still present, is commonly masked because many unconnected vadose passages terminate in sumps, collapse material, or perched springs. Because of high relief and intense fracturing, the water table may lie more than 1,000 m below the surface. The deepest known caves in the world, with vertical extents as much as 1,600 m, are located in mountain ranges such as the Pyrenees and the Alps.

ORIGIN AND MODIFICATION OF CAVES BY FLOOD WATER

Characteristics of Flood-water Recharge

Caves fed by sinking streams are exposed to intense flooding during periods of high rainfall or snowmelt. Rapid infiltration in large catchments of bare alpine karst and bank-flooding adjacent to rivers can have a similar effect. During periods of high runoff into open depressions, the water level in major cave passages rises faster than in surrounding fractures and pores. The normal hydraulic gradient toward the passages is

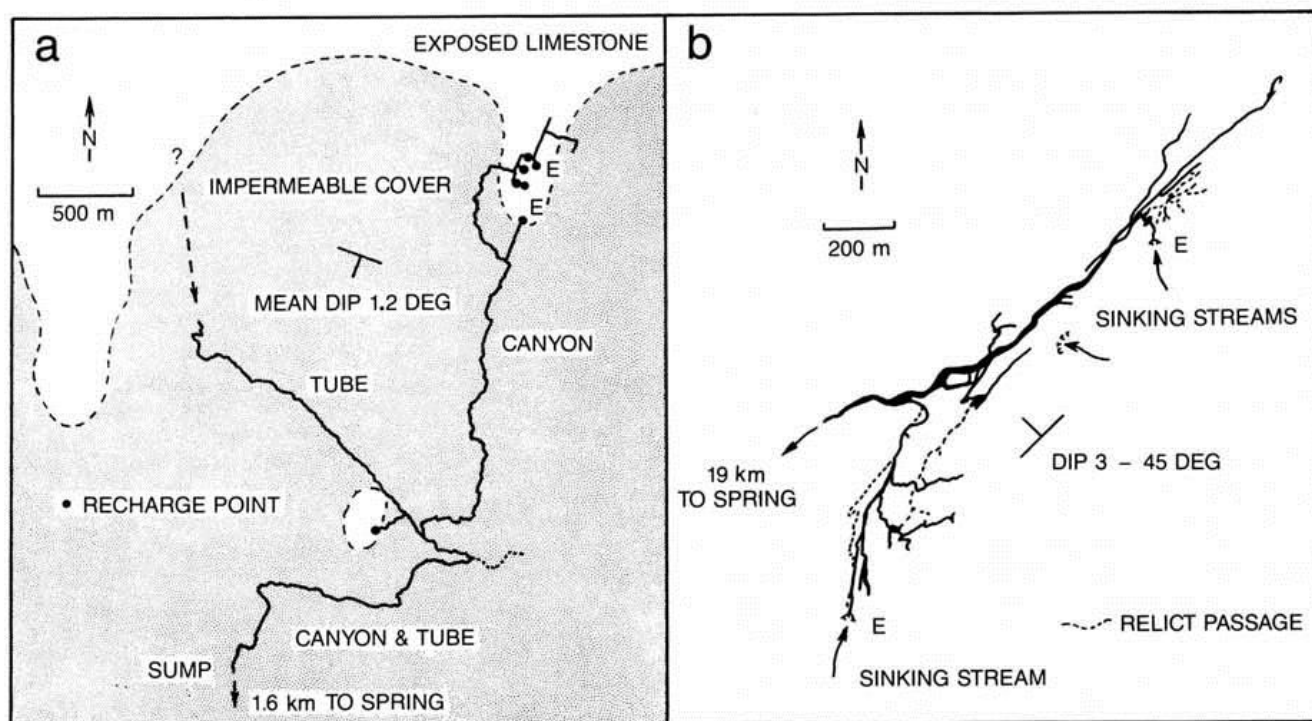


Figure 19. Stratigraphic and structural influence on branchwork caves: (a) Map of McFall's Cave, New York, showing how an insoluble caprock limits recharge without interfering with the branchwork pattern (map by A. N. Palmer, E. H. Kastning, and J. Schweyen); (b) Ludington Cave, West Virginia, showing the effect of steeply dipping beds (map courtesy of West Virginia Association for Cave Studies).

temporarily reversed, and water is injected under steep hydraulic gradients into adjacent openings. This process is most extreme where an active passage contains local impediments of collapse debris, insoluble beds, or sediment fill (Palmer, 1972, 1975).

The head loss across such a constriction varies with the square of the discharge. Flooding can produce discharges several orders of magnitude greater than that of low flow; water therefore readily ponds on the upstream side of each constriction. In some areas, peak flows of several tens of cubic meters per second in a single conduit are fairly common. Overflow of flood water from cave streams into higher-level openings, and its eventual slow release, can attenuate flood peaks at karst springs (Mangin, 1975).

The water-table rise during a flood can be viewed as a temporary return of phreatic conditions to otherwise vadose domains; but the resulting processes are quite different from those of normal phreatic water. Hydraulic gradients and flow rates are larger, and the water is much more aggressive. Caves grow rapidly at or near the maximum rate shown at the tops of the graphs in Figure 12. Values of i/L greater than 0.001 cm^{-1} are common, especially where collapse has nearly obstructed an active stream passage. From Figures 12 and 13, it is apparent that in these conditions all fractures wider than about

0.005–0.01 cm will enlarge at or near the maximum possible rate without having to pass through an initial phase of slow dissolution. If all competing openings are fed by the same water source, they have virtually identical C_0 and C_s values. Simultaneous enlargement of many openings produces a maze of intersecting passages. Although flood-water processes operate only during a small part of the year, they involve such intense dissolution and abrasion that, under favorable conditions, traversable passages can form in less than 10,000 yr.

Flood-water features include *injection features* formed by bank storage adjacent to flood-prone passages or surface rivers, and *diversion conduits* that transmit flood water around passage constrictions. Many caves contain a combination of both, and the first type often develops into the second. These features are subdued or absent in efficiently drained caves, or where recharge varies only slightly with time. At least 10% of the caves in the observed sample, both in number and length, show considerable modification by flood-water dissolution.

Flood-water Injection Features

Under normal flow conditions, most of the fractures and partings adjacent to a cave are either air filled or contain water at or near chem-

ical saturation. When a cave floods, aggressive water is forced into these openings and is released slowly as the flood subsides. They enlarge rapidly into solution pockets and dead-end fissures such as those shown in Figure 6. These features are most common in the cave walls and ceiling, where shielding by detrital sediment is minimal. Where fractures are prominent and flooding is severe, network mazes can form. An entire cave may be a maze if it is fed by bank storage from a surface river. More commonly, mazes are superposed on pre-existing branchwork caves. Skull Cave, New York, in the Devonian Helderberg Group, contains several network mazes that emanate laterally and upward from the stream passages (Palmer, 1975). The mazes, with an aggregate length of 4 km and containing individual fissures up to 500 m long, were formed by periodic flood waters ponded by a stratigraphic trap and glacial till.

In prominently bedded rock, the most common flood-water injection features are bedding-plane anastomoses. These are small interconnected tubes similar in pattern to anastomotic mazes, except that the openings diminish in size away from the source passage, show no evidence of high-velocity flow, and are rarely of traversable size. Most authors consider them to be relics of the initial stage of cave origin. Unless they are fed by a nearby aggressive water source,

however, proto-cave openings contain water close to saturation and are more likely to form unitary conduits. The uniform enlargement rate necessary to form anastomoses is more easily achieved by flood water.

In conglomeratic or massive carbonate rocks with high intergranular porosity, flood-water ponding may form spongework in the cave walls. Fine examples occur in Big Brush Creek Cave, Utah, in the brecciated limestone of the Mississippian Humbug Formation (Palmer, 1975). Like anastomoses, spongework of this origin is rarely of traversable scale.

Flood-water Diversion Conduits

Short constrictions in an active stream passage are generally bypassed by a maze of diversion passages, either network, anastomotic, or (rarely) spongework, depending on the bedrock structure. Similarly, collapse or detrital blockage of a cave spring produces a distributary system of fissures or tubes bypassing the blockage and feeding overflow springs (Palmer, 1984a). Single-conduit bypasses are also common, but they usually have irregular cross sections modified by flood-water injection.

A flood-water maze bypassing a constriction originates as injection features that quickly evolve into through-flow conduits. This process can be remarkably fast, as shown by the maximum rates in Figure 12. It might seem that only one or two bypass routes would be sufficient to transmit the flow. Even the bypass conduits, however, contain steep hydraulic gradients during floods. Head loss is highly sensitive to passage size (eqs. 3 and 4), and so even slight size variations cause great differences in head between adjacent conduits, allowing interconnections to form. Fissures and pockets formed by

flood-water injection complicate the pattern and may eventually connect adjacent bypass conduits. A maze is therefore more common in this situation than a single diversion conduit or several parallel ones.

A fine example of a flood-water diversion network is located in Blue Spring Cave, a predominantly branchwork cave in massive jointed limestone (Fig. 16a). Late in the evolutionary history of the cave, collapse at a passage junction caused water to pond upstream during floods and form a 2-km-long maze of passages bypassing the blockage. The maze consists of intersecting fissures with a vertical range of 20 m. Some are perennially water filled, and others fill completely during floods. The acute and obtuse angles of many passage intersections, which contrast with the nearly right-angle pattern elsewhere in the cave, are typical but not necessarily diagnostic of networks of this origin. This joint pattern may result from release of stress during collapse. Further collapse is promoted by flood-water dissolution and erosion.

Examples of anastomotic flood-water mazes are shown in Figures 4, 6, and 16b, where chert beds constrict the main cave passages. A braided pattern of synchronously formed tubes paralleling the main passage is typical. Many anastomotic mazes do not bypass distinct constrictions but merely provide alternate routes for flood water when it fills the main passage (Fig. 16b).

The bare bedrock surface of alpine karst allows rapid ground-water recharge. Alpine caves that drain a large surface area are highly flood prone, and their patterns tend to be complicated by flood-water features. The world's largest alpine cave, Hölloch, in Switzerland, with 150 km of passages, is largely anastomotic. A partial map is shown in Figure 1c (see also Bögli, 1970). Short-term rises in head often exceed 100

m. Although the cave developed at several distinct levels as the base level dropped, it has been integrated into a single maze (except for vadose passages high in the system) because the annual flood range exceeds the spacing between levels.

ORIGIN OF MAZE CAVES BY DIFFUSE RECHARGE

Caves can be formed by diffuse recharge through intergranular pores in soluble rock or through overlying or underlying rock that is permeable but insoluble. Such caves are almost all network or spongework mazes, depending on whether fractures or intergranular pores are dominant (Palmer, 1975).

Diffuse Infiltration into Porous Limestone

Water infiltrating directly into limestone of high intergranular porosity quickly approaches saturation. This water rarely forms caves because its aggressiveness is lost within a few meters of the surface. Caves form at depth, however, if the water regains its aggressiveness by mixing with water from another source of different chemistry. Usually the difference is in either CO_2 content (Bögli, 1964), salinity (Wigley and Plummer, 1976), or H_2S content. Mixing of fresh ground water with sea water in coastal aquifers theoretically produces an aggressive mixture at certain ratios (Plummer, 1975). This process has been measured in Bermuda by Plummer and others (1976) and in the Yucatan by Back and others (1984). Palmer and others (1977) showed the aggressiveness in Bermuda caves to be enhanced more by differences in CO_2 than in salinity.

Figure 20 shows the saturation values for calcite and dolomite on a linear scale as a function of equilibrium CO_2 or H_2S at 25 °C. At lower temperatures, dolomite cannot reach saturation without driving calcite to supersaturation, causing incongruent dissolution. Calculations for pure H_2S assumed that any CO_2 generated by the reaction with carbonates is retained in solution. When two saturated solutions (A and B) mix, the resulting solution (C) is undersaturated with respect to calcite or dolomite. The system is closed, and so dissolution of each additional mole of calcite consumes a mole of CO_2 or H_2S . Each mole of dolomite consumes two of CO_2 or H_2S . The second dissociation of carbonic and hydrosulfuric acid is negligible except at high pH, and so each essentially donates only a single proton. Each millimole of gas is therefore able to dissolve $\sim 0.037 \text{ cm}^3$ of calcite or $\sim 0.032 \text{ cm}^3$ of dolomite. The final saturation value of calcite for mixtures is found by projecting a line of slope -0.037 (-0.032 for dolomite) from the mixing point (C) to the saturation curve (D).

Dissolution by mixing is favored by a large

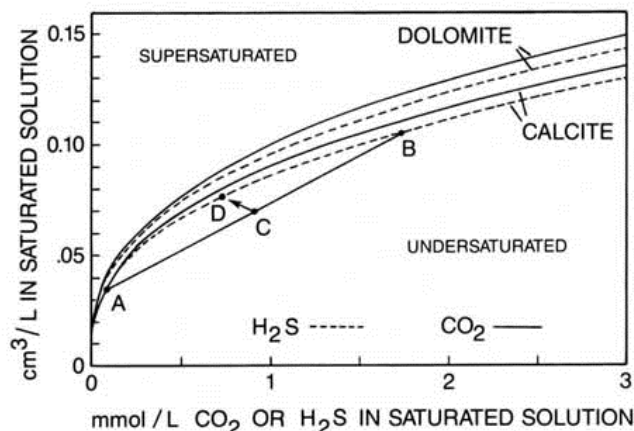


Figure 20. Saturation concentration of calcite and dolomite as a function of CO_2 or H_2S concentration, in volume of dissolved solid per liter, calculated in the same manner as Figure 7. Mixing of two saturated solutions (for example, A and B) produces an undersaturated solution (C). Subsequent dissolution follows line C-D. See text for details.

difference in equilibrium gas content between the two solutions, especially if one gas concentration is very low. If the flow rates of the two sources are known, the annual increase in pore volume can be estimated from a simple mass balance without regard for kinetics, because most of the aggressiveness appears to be consumed at and near the mixing site. For this reason, Figure 20 shows volumetric rather than mass concentration, to allow more direct field application. Values for discharge and C_s are not easily obtained, and they tend to vary with season, rainfall, or tides. Two water sources rarely mix in nearly equal proportion. Usually one is much less abundant, and its rate of inflow into the larger source controls the dissolution rate. In small openings with laminar flow, mixing takes place mainly by diffusion of chemical species, rather than by hydraulic mixing.

Caves of mixing origin represent 8%–10% of the sample number but less than 3% of the total length. Typical patterns are shown by Palmer (1984a) and Mylroie (1988) and are summarized in the diagram at the end of this paper. Most are spongeworks, networks, or irregular rooms modified by breakdown and travertine. Individual solutional pores are strongly aligned along bedding or fractures but collectively tend to form tabular zones limited to the areas of most intense mixing. Subhorizontal spongework in porous seacoast limestones indicates former stands of Pleistocene sea level, where fresh infiltrating water mixed with sea water. Mylroie (1988) described cave origin in the Bahamas at both the vadose/phreatic mixing zone and the fresh-water/salt-water interface. Caves are subhorizontal in the former zone and inclined downward away from the coast in the latter. Most Bahamian caves form close to, and subparallel to, the coastline, where groundwater flow and mixing are greatest. Some are crude branchworks formed by converging water, but most branches terminate headward and cannot be followed to their diffuse sources. The karst surface is highly porous, but few of the openings connect via traversable solutional routes to underlying caves. Access to most caves is through collapse sinkholes or at random intersections with the eroded land surface.

Recharge through Permeable Insoluble Rocks

Of the network caves in the observed sample, 75% are capped by thin permeable sandstone. Where these same sandstones are thicker or grade laterally into less permeable facies, the underlying caves, if any, have a branchwork pattern (Palmer, 1975). In upland settings, the sandstone transmits aggressive but diffuse recharge to the underlying limestone. All major fractures in the limestone receive nearly uniform recharge of similar chemistry, allowing them all

to grow at comparable rates (Fig. 12b). About 5% of the caves in the sample (7% of the total length) show evidence that they were formed, or at least initiated, in this way.

Fracture enlargement may begin while the sandstone/limestone contact is below fluvial base level. Initially the sandstone has the greater permeability, and most of the ground water flows through it. The small amount of water entering the limestone gradually widens fissures solutionally, however, until the limestone acquires the higher permeability. Much or most of the water then flows through the limestone, as the total resistance to flow is less than in the sandstone alone. Discharge to each fissure varies logarithmically with fissure width and so is rather insensitive to width variations (Palmer, 1975). All fissures receive comparable amounts of flow regardless of width, and they grow at similar rates. This process continues after the cave becomes air filled.

For example, Crossroads Cave, Virginia (Fig. 1b), in the Devonian Helderberg Group, is capped by thin Oriskany Sandstone. It contains a rectilinear network section in which aggressive recharge still enters through the sandstone, modifying the cave walls with vertical flutes. Most caves of this type, however, are exposed at the surface by fluvial entrenchment and are greatly enlarged by flooding from adjacent rivers after the skeletal outline of the caves has been established by diffuse infiltration. The zone of maximum enlargement is therefore not necessarily immediately below the sandstone.

Much of the water infiltrating through an insoluble caprock is isolated from soil carbon dioxide. When it reacts with carbonates within or below the caprock, it does so under nearly closed conditions, so that little carbonate can be dissolved and the equilibrium P_{CO_2} decreases to a very low level (see Figs. 7 and 11). When this water mixes with ground water from other sources, the disparity in CO_2 concentration can be very large, and the renewed aggressiveness is likewise large (Fig. 20).

In many sandstone-capped network caves, the water is channeled through joints in the caprock that are co-planar with those in the limestone. In this case, the soil governs the flow to each joint. If diffuse flow encounters poorly jointed limestone, interstratal dissolution and complex systems of shafts and narrow canyons are common.

THE QUESTION OF ARTESIAN MAZE CAVES

Maze caves are often attributed to slow flow deep within artesian aquifers. Some of the world's largest network caves, including Wind and Jewel Caves in the Black Hills (Fig. 3), are located in carbonate rocks that extend down-dip into confined settings. In artesian carbonate aquifers that rise enough at the downstream end

to allow rapid through-flow to karst springs, however, diving usually reveals discrete tubular passages. The main question is whether network mazes can form in the nearly stagnant water of an artesian aquifer that has no efficient outlet.

Figure 21 shows a simple loop, the fundamental element of an incipient maze, in which water diverges into two branches (1 and 2) that rejoin downstream. Under what conditions will the two branches enlarge at similar rates to form a traversable closed loop? The growth rate of either branch is governed by equations 2 and 7. The graphs in Figure 21, determined from equations 3, 6, and 7, show relative enlargement rates between the branches as a function of C_0/C_s at the upstream end of the loop and q/L in the wider branch. For simplicity, each branch is considered to have the same fissure length (L) and height (b), and so differences in growth rate depend only on differences in the effective widths (and therefore q) in the two branches. Gains or losses at intermediate junctions along the length of either branch of such a loop are neither consistently positive nor negative and so are ignored.

The two branches will grow at similar rates only if the ratio of solution rates is in the vicinity of 1.0. Unless the two branches fortuitously have identical effective widths, this condition is met only at very high C_0/C_s or q/L (Fig. 21). Otherwise the enlargement rate in the wider branch is greater than that in the narrower branch by a factor whose maximum value is equivalent to $(w_2/w_1)^3$, where w_2 is the larger effective width. In a typical aquifer, owing to the great variety of fracture widths and lengths, one branch in such a loop is likely to enlarge much faster, decreasing the hydraulic gradient and diminishing the flow in the narrower one. At best, only a few isolated cave loops can be expected. At $q/L > 10^{-3}$ cm/sec, the two branches are competitive at any value of C_0/C_s , but such a high q/L is normally achieved only in flood-water conditions. In a typical artesian aquifer, q/L ranges from about 10^{-8} to 10^{-10} cm/sec. Under these conditions, the two branches are competitive only at saturation ratios so high that a traversable cave could not form within a geologically feasible time. Evidently the slow rates of flow and dissolution typical of an artesian aquifer are *least* likely to form closed loops. Maze caves in artesian aquifers must originate by some other mechanism, either by diffuse recharge through insoluble semi-confining beds, or by simultaneous production of aggressiveness along many alternate flow routes. The latter process is discussed below.

HYPOGENIC CAVES

Fewer than 10% of the caves in the observed sample have a proven or suspected hypogenic origin, but they include some of the world's

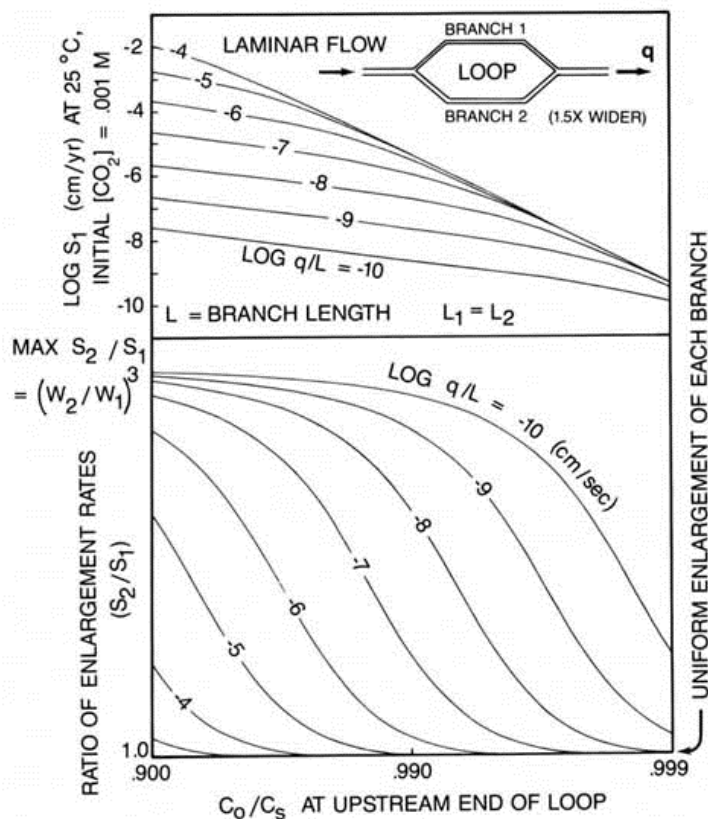


Figure 21. Comparison of enlargement rates between the branches in a closed loop, where branch 2 is 1.5 times wider than branch 1. Both branches are equal in length (L) and height (b). Values for q/L are those in the wider branch. The two branches have similar growth rates only at high q/L , typical of flood water rather than artesian conditions.

largest. Examination of drill cores indicates that accessible caves represent only a tiny fraction of the porosity formed in this way. The most abundant hypogenic acids are carbonic acid and hydrosulfuric acid (aqueous hydrogen sulfide). Solutional pores and caves form where these acids move from insoluble rocks into carbonate rocks, or where water becomes aggressive because of mixing, oxidation of H_2S , or a drop in temperature. The last three processes are the most important in forming hypogenic caves.

Mixing of H_2S -rich Waters

Renewed aggressiveness caused by the mixing of waters of different H_2S content is shown in Figure 20. This process is probably more important to the evolution of carbonate petroleum reservoirs than to cave origin. Solutional caves filled with stagnant H_2S -rich water have been encountered in mines (Warwick, 1968). Some are associated with hydrothermal ores, such as those in lead-zinc mines in the Picher Field of Oklahoma-Kansas (McKnight and Fischer, 1970). It is not certain whether most such caves

cally by hydrothermal processes or reduction of sulfates.

Oxidation of Sulfides

Sulfuric acid can form directly or indirectly by the oxidation of H_2S . It has been shown to form caves where aqueous or gaseous H_2S rises to the water table from sedimentary basins (Egemeier, 1981; Davis, 1980; Hill, 1987). The sulfide-rich fluids are either released slowly over long time periods by deep circulation of meteoric water or rapidly in short-term events. The latter can include migration of basin brines into marginal areas by compaction of sediments, rising of fluids in thermal plumes generated by igneous activity, or release of deep-seated water and gases from overpressured zones by hydraulic fracture or tectonic activity.

Figure 22 shows the saturation concentration of calcite in H_2S and H_2SO_4 solutions at 25 °C. It is assumed that the water is first saturated with calcite below the water table in the presence of H_2S and CO_2 ; then when the water rises to the water table, all H_2S oxidizes to H_2SO_4 , and a

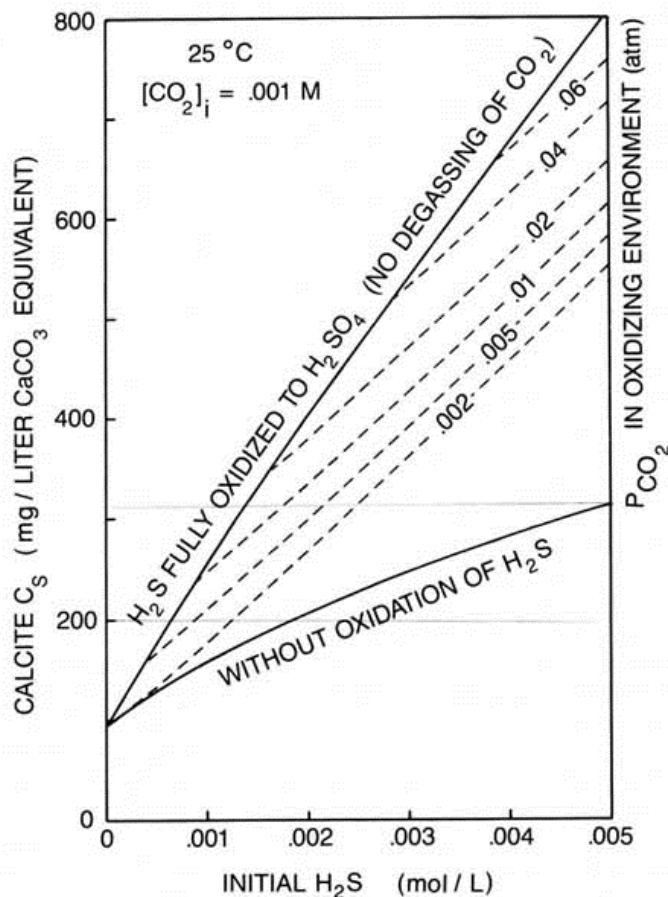


Figure 22. Dissolution of calcite in an H_2S - H_2SO_4 system at $[CO_2]_i = 0.001$ M (calculated in the same manner as Fig. 7).

aqueous CO_2 concentration, $[CO_2]_i$, of 0.001 M (44 mg/L) is assumed. Conversion of H_2S to H_2SO_4 provides a sudden burst of dissolution, but the effect is attenuated if there is degassing of CO_2 generated by the H_2SO_4 - $CaCO_3$ reaction. As in other mixing situations, a simple mass balance is perhaps the best way to quantify dissolution rates, because the undersaturation depends on too many uncertain variables to allow calculation of meaningful rates via kinetic equations. Large rooms and corridors form at the water table, as in Carlsbad Cavern (Figs. 1d and 5). Narrow fissures in their floors, now clogged with secondary deposits, represent the original upward paths for H_2S -rich water. A single conduit forms where water enters at one point and flows rapidly to a spring (Egemeier, 1981). Diffuse inflow to many intersecting fissures may form a network. Regardless of the nature of the input, if the water becomes sufficiently undersaturated, numerous alternate flow routes can be enlarged at comparable rates, as in a flood-water cave, forming networks and spongework.

If the concentration of dissolved sulfate is great enough, it can replace the limestone wall

tals on the walls of the Kane Caves along the Sheep Mountain Anticline in Wyoming have formed in this way (Egemeier, 1981). In contrast, massive gypsum blocks in caves in the Guadalupe Mountains of New Mexico are primary deposits formed in water supersaturated with calcium sulfate soon after the main phase of cave dissolution (Davis, 1980; Hill, 1987).

Certain cave rooms show evidence for having been enlarged or modified by H_2S that has degassed from underlying water and which rises into cave pools having no outlet. Oxidation to H_2SO_4 allows dissolution of limestone in and above the pool, releasing CO_2 . After the acid has been neutralized, the final C_s of the water depends on the P_{CO_2} of the air above the pool. If the P_{CO_2} returns to its original value, the water tends to precipitate the limestone dissolved by the H_2S and H_2SO_4 . The cave room is enlarged at and above the pool level, but the floor and ascending fissures are occluded by carbonate precipitates. The local cave volume may show no net increase.

Sulfuric acid is also produced by oxidation of pyrite, but the process is usually too slow and the pyrite too dispersed to create more than local pores. A few small caves have been attributed to this process (Morehouse, 1968).

Dissolution by Rising Thermal Water

Because of the inverse relationship between calcite solubility and temperature, even at constant CO_2 levels (Fig. 7), decreasing temperature in rising thermal waters can maintain or create solutional aggressiveness. To test the effectiveness of this process, finite-difference analyses were conducted in which CO_2 -rich water was allowed to rise through a 100-m-long fissure in limestone, cooling in the direction of flow. The water was assumed to be completely saturated with calcite when it began to rise. The fissure was divided into 100 uniform length increments, and the dissolution rate in each was calculated using equations 2 and 7 with $n = 4$, and k adjusted continuously as the saturation level changed (see Table 1). The change of C_s with temperature was determined with the equations for equilibrium constants given by Plummer and Busenburg (1982). Within the range of k and n values in Table 1, the shapes of the resulting graphs were so consistent that it seemed justifiable to extrapolate their trends to 50 °C to simulate distinctly thermal waters.

Figure 23 shows the results of several runs with temperature drops from 50 to 45 °C and from 25 to 20 °C at $[CO_2]_i = 0.005$ M (220 mg/L). These conditions are typical of the well-documented thermal caves of Budapest (Takács-Bolner and Kraus, 1989), although

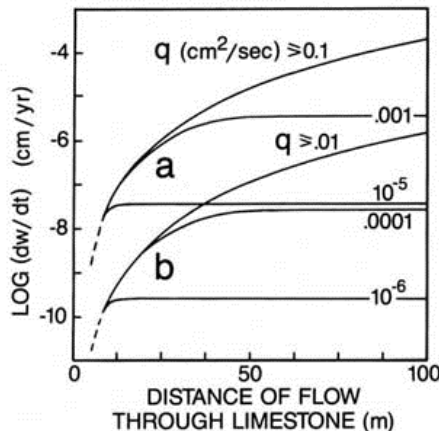


Figure 23. Rate of fissure widening by rising thermal water: (a) cooling from 50 to 45 °C and (b) from 25 to 20 °C. $[CO_2]_i = 0.005$ M.

mixing with shallow ground water enhances the development of those particular caves. Solutional widening rates increase in the direction of flow, leveling off to constant values only at very small discharge. The low C_s at high temperatures is offset by large k values, causing enlargement rates to increase with temperature. Doubling either the thermal gradient or $[CO_2]_i$ allows a potential increase in growth rate of approximately ten times, with no change in the shape of the curves. No rate increase can be fully realized without a proportional increase in q , however. Most significantly, increasing q causes the enlargement rate to reach a maximum curve, beyond which any further increase in q has no effect. As a result, enlargement of fissures by cooling water reaches a maximum rate that is independent of discharge. Regardless of their size or flow, if many fissures receive thermal water of similar character, they will all enlarge at the same rate, forming a network maze. Such networks as Wind Cave in the Black Hills may have been formed or modified by this process (Fig. 3; Bakalowicz and others, 1987).

Only under the most favorable conditions can dissolution by cooling of thermal water produce caves of traversable size. Even then, times on the order of 10^5 to 10^6 yr are required. Most thermal cave origin probably requires the presence of hypogenic acids or mixing with meteoric water from nearby sources. Soil-derived CO_2 alone rarely exceeds 0.0025 M, which would provide growth rates only 10% of those in Figure 23.

The equilibrium P_{CO_2} of rising water is usually greater than that of the atmosphere of the cave into which it emerges. Degassing of CO_2 takes place as the pressure drops, causing calcite to precipitate. This process is usually limited to

depths within a few meters of the water table, and so precipitation of calcite rapidly diminishes with depth and gives way to bedrock dissolution.

Recognition of Inactive Hypogenic Caves

Most accessible hypogenic caves are now inactive relics whose origin must be deduced indirectly. The main clue is a lack of genetic relationships to recharge from overlying or immediately adjacent surfaces. Most entrances are random intersections of the caves by surface erosion, mining, or quarrying. Nearly all ramiform caves appear to be hypogenic. Network, spongework, and single-passage caves are also common. True branchwork patterns are virtually non-existent. Anastomotic caves can form in highly acidic water, particularly in zones of H_2S oxidation. Cave profiles are highly irregular, except where aggressive water rises to the water table and flows laterally along it. Variations in cross section are extreme, and cave ceilings may contain rounded, dome-like alcoves. Solutional scallops and coarse detrital sediment are rare and generally represent invasion by surface water.

Air and water flow between entrances at different levels, typical of epigenic caves, is lacking in most hypogenic caves. Thermal gradients are therefore high in the latter, and it is common for warm moist air to rise from deep passages and cause moisture to condense on the colder surfaces of upper-level passages. Condensation water formed in the CO_2 -rich air of a cave is very aggressive. Surfaces exposed to condensation exhibit high porosity and a friable weathering rind. The water generally seeps back to lower levels by capillary and gravity flow, where it evaporates once more, depositing its dissolved load as speleothems. These evaporative deposits typically include botryoidal calcite, aragonite needles, and hydrated carbonate minerals. Floor sediment consists mainly of powdery, disintegrated carbonate rock and insoluble residue. Crystal linings of calcite deposited by CO_2 degassing from water surfaces may coat the bedrock walls of lower levels, as at Jewel Cave and parts of Carlsbad Cavern. Such deposits are commonly low in $^{18}O/^{16}O$ relative to other cave calcites (Bakalowicz and others, 1987).

Hypogenic cave patterns, like those of epigenic caves, are controlled by the mode of recharge to the soluble rock. Single-passage caves and simple ramiform caves are formed by point sources of recharge entering the soluble rock from below. Network, spongework, and complex ramiform patterns are formed by diffuse flow through underlying insoluble rocks, renewal of aggressiveness within numerous joints by mixing or oxidation, and decreasing temperature of

rising water within a large number of unenlarged fissures. Some hypogenic networks, like their epigenic counterparts, appear to have achieved only their initial growth through these processes, with most of their enlargement by water from other sources that alone would not have formed networks.

Hicks Cave, near Carlsbad, New Mexico, is a typical hypogenic cave formed by H_2S and H_2SO_4 (Fig. 24). Its profile is irregular, with little regard for topography or lithology. It has a ramiform pattern with several sequential levels of development, each with a different outlet direction (Fig. 24): (1) an irregular tube rising into overlying Fence Canyon at a level now several tens of meters above the valley bottom; (2) a major level of rooms, apparently formed along a zone of H_2S oxidation at the water table, with an outlet in a new direction toward the Guadalupe Escarpment; (3) two intermediate levels of complex rooms, with outlets in uncertain directions; and (4) low-level fissures, now choked with carbonate sediment, which apparently functioned as the inlet for H_2S -rich water throughout all phases of cave development. The cave is now entirely relict.

Inactive hypogenic caves are most difficult to distinguish in a humid climate. Invading surface water tends to overwhelm the deep-seated processes, or to modify the caves so that their pre-existing hypogenic features are masked. In arid areas, where the inflow of water is minimal, hypogenic caves can survive with little modification by surface processes. In humid climates, there must be many caves initiated by deep-seated processes that have not yet been suspected of having such an origin. Prime candidates are certain network caves in the Appalachians that show no evidence for flood water or diffuse recharge. One of the major goals of future cave research will be to identify the relative influence of shallow versus deep processes in such areas.

CONCLUSIONS

The morphology of a cave is controlled by a hierarchy of influences: (1) Its location, extent, and over-all trend are controlled by the distribution of soluble rocks and of recharge and discharge points. (2) The passage pattern (for example, branchwork or maze) depends on the mode of ground-water recharge. (3) The orien-

tation of individual passages is controlled by the geologic structure, distribution of vadose and phreatic flow, and geomorphic history. A typical cave passage develops in two stages: a lengthy period of slow dissolution near saturation, followed by rapid dissolution at lower saturation ratios. The time required for the cave to complete its first stage of development varies directly with flow distance and temperature and inversely with discharge and P_{CO_2} . It is only slightly dependent on chemical kinetics. Later rapid growth rates, however, depend mainly on kinetics. Branchwork caves are formed by recharge through an overlying or adjacent karst surface, which evolves in conjunction with underground conduits. Maze caves, formed by the simultaneous enlargement of many competing openings, require either (1) steep hydraulic gradients and low saturation ratios, as in caves exposed to flood waters; (2) uniform recharge to many fissures in soluble rock through an adjacent porous but insoluble formation; or (3) uniform production of aggressiveness in each fissure, as in rising thermal water. Condition 1 also accounts for the numerous interconnecting solutional openings in the epikarst.

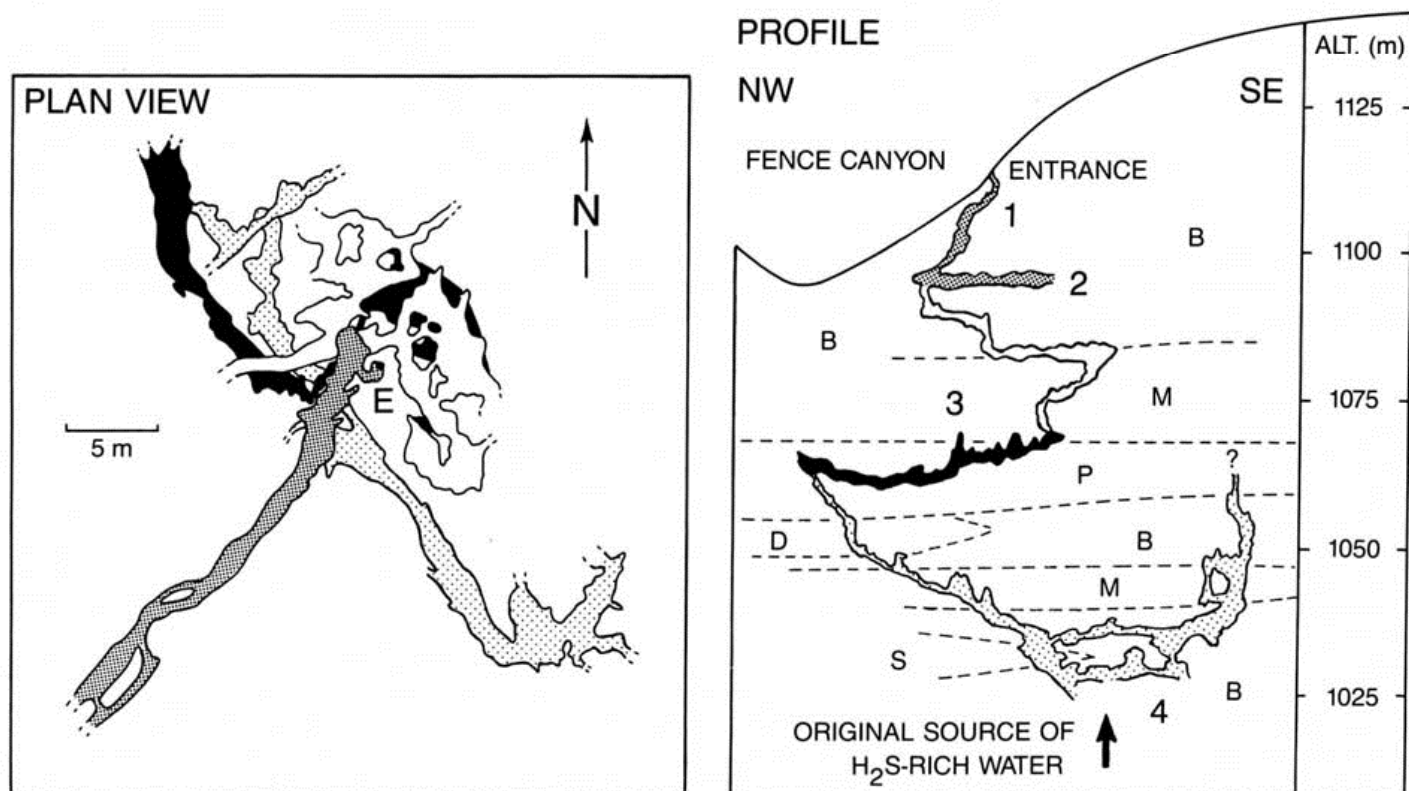


Figure 24. Map and profile of Hicks Cave, New Mexico, a hypogenic cave in Permian back-reef carbonate rocks (no vertical exaggeration). About half the surveyed passages have been omitted for clarity. B = carbonate breccia; M = micritic limestone and dolomite; P = pisolitic limestone; S = silty limestone and dolomite. Numbers refer to stages of development described in text. Plan view from surveys by the Cave Research Foundation. Profile by M. V. Palmer.



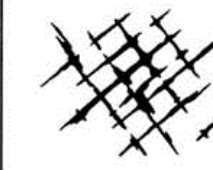
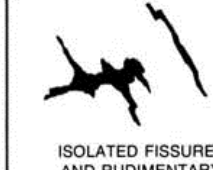



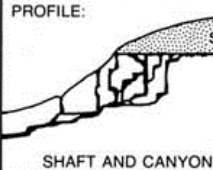


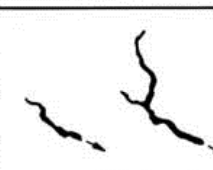

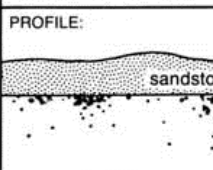


		TYPE OF RECHARGE				
		VIA KARST DEPRESSIONS		DIFFUSE		HYPOGENIC
		SINKHOLES (LIMITED DISCHARGE FLUCTUATION)	SINKING STREAMS (GREAT DISCHARGE FLUCTUATION)	THROUGH SANDSTONE	INTO POROUS SOLUBLE ROCK	DISSOLUTION BY ACIDS OF DEEP-SEATED SOURCE OR BY COOLING OF THERMAL WATER
		BRANCHWORKS (USUALLY SEVERAL LEVELS) & SINGLE PASSAGES	SINGLE PASSAGES AND CRUDE BRANCHWORKS, USUALLY WITH THE FOLLOWING FEATURES SUPERIMPOSED:	MOST CAVES ENLARGED FURTHER BY RECHARGE FROM OTHER SOURCES	MOST CAVES FORMED BY MIXING AT DEPTH	
DOMINANT TYPE OF POROSITY	FRACTURES	 ANGULAR PASSAGES	 FISSURES, IRREGULAR NETWORKS	 FISSURES, NETWORKS	 ISOLATED FISSURES AND RUDIMENTARY NETWORKS	 NETWORKS, SINGLE PASSAGES, FISSURES
	BEDDING PARTINGS	 CURVILINEAR PASSAGES	 ANASTOMOSES, ANASTOMOTIC MAZES	PROFILE:  SHAFT AND CANYON COMPLEXES, INTERSTRATAL SOLUTION	 SPONGEWORK	 RAMIFORM CAVES, RARE SINGLE-PASSAGE AND ANASTOMOTIC CAVES
	INTERGRANULAR	 RUDIMENTARY BRANCHWORKS	 SPONGEWORK	PROFILE:  RUDIMENTARY SPONGEWORK	 SPONGEWORK	 RAMIFORM & SPONGEWORK CAVES

Figure 25. Summary of cave patterns and their relationship to types of recharge and porosity. Maps are plan views unless otherwise noted and are generalized to represent typical caves in each category. Many exhibit rudimentary forms, multiple stages of development, or combinations of more than one type. Individual passages differ in specific layout according to the local physical setting.

Cave patterns are summarized in Figure 25 in relation to the recharge and geologic conditions that control them. Each category includes several stages of development: rudimentary single passages, caves with fully developed patterns from a single stage of development, and multi-stage caves consisting partly or entirely of inactive relict passages in which the basic morphology is obscured by interconnecting passages of different age. Solutional caves are far more diverse in origin and morphology than is generally realized, and the processes that form them play a significant role in many geologic fields.

ACKNOWLEDGMENTS

I thank Margaret V. Palmer for her contribution to the mapping, field work, and laboratory analyses on which many of the ideas in this

paper are based. Field work was supported in part by the Research Foundation of the State University of New York. The National Park Service and Cave Research Foundation provided facilities and assistants in various national parks and monuments. Many thanks to Derek C. Ford, Henry W. Rauch, William B. White, and Noel Krothe for helpful editorial suggestions.

REFERENCES CITED

- Atkinson, T. C., 1977, Carbon dioxide in the atmosphere of the unsaturated zone: An important control of ground-water hardness in limestones: *Journal of Hydrology*, v. 35, p. 111-123.
- Back, W., Hamshaw, B., and Van Driel, J. N., 1984, Role of groundwater in shaping the eastern coastline of the Yucatan Peninsula, Mexico, in LaFleur, R. G., ed., *Groundwater as a geomorphic agent*: Boston, Allen and Unwin, Inc., p. 281-293.
- Bakalowicz, M. J., Ford, D. C., Miller, T. E., Palmer, A. N., and Palmer, M. V., 1987, Thermal genesis of dissolution caves in the Black Hills, South Dakota: *Geological Society of America Bulletin*, v. 99, p. 729-738.
- Berner, R. A., and Morse, J. W., 1974, Dissolution kinetics of calcium carbonate in sea water, IV: Theory of calcite dissolution: *American Journal of Science*, v. 274, p. 108-134.
- Böcker, T., 1969, Karstic water research in Hungary: *International Association of Scientific Hydrologists Bulletin*, v. 14, p. 4-12.
- Bögli, A., 1964, Mischungskorrosion, ein Beitrag zur Verkarstungsproblem: *Erdkunde*, v. 18, p. 83-92.
- 1970, *Le Hölloch et son karst*: Neuchâtel, Editions de la Baconnière, 109 p.
- Bray, L. G., 1972, Preliminary oxidation studies on some cave waters from south Wales: *Cave Research Group of Great Britain, Transactions*, v. 14, p. 59-66.
- Bretz, J. H., 1942, Vadose and phreatic features of limestone caverns: *Journal of Geology*, v. 50, p. 675-811.
- Buhmann, D., and Dreybrodt, W., 1985a, The kinetics of calcite solution and precipitation in geologically relevant situations of karst areas. 1: Open system: *Chemical Geology*, v. 48, p. 189-211.
- 1985b, The kinetics of calcite dissolution and precipitation in geologically relevant situations of karst areas. 2: Closed system: *Chemical Geology*, v. 53, p. 109-124.
- Busenberg, E., and Plummer, L. N., 1982, The kinetics of dissolution of dolomite in CO_2 - H_2O systems at 1.5 to 65° C and 0 to 1 atm P_{CO_2} : *American Journal of Science*, v. 282, p. 45-78.
- Courbon, P., and Chabert, C., 1986, *Atlas des grandes cavités mondiales*: Paris, Union Internationale de Spéléologie et Fédération Française de Spéléologie, 255 p.
- Coward, J. M. H., 1975, Paleohydrology and streamflow simulation of three karst basins in southeastern West Virginia [Ph.D. thesis]: Hamilton, Ontario, McMaster University, 394 p.
- Curl, R. L., 1968, Solution kinetics of calcite, in *International Congress of Speleology*, 4th, Ljubljana, Yugoslavia, Proceedings, p. 61-66.
- Davis, D. G., 1980, Cave development in the Guadalupe Mountains: A critical review of recent hypotheses: *National Speleological Society Bulletin*, v. 42, p. 42-48.
- Davis, W. M., 1930, Origin of limestone caverns: *Geological Society of America Bulletin*, v. 41, p. 475-628.
- Dreybrodt, W., 1981a, Kinetics of the dissolution of calcite and its applications

- to karstification: *Chemical Geology*, v. 31, p. 245-269.
- 1981b, Mixing corrosion in $\text{CaCO}_3\text{-CO}_2\text{-H}_2\text{O}$ systems and its role in the karstification of limestone areas: *Chemical Geology*, v. 32, p. 221-236.
- 1987, The kinetics of calcite dissolution and its consequences to karst evolution from the initial to the mature state: *National Speleological Society Bulletin*, v. 49, p. 31-49.
- 1988, Processes in karst systems: Physics, chemistry, and geology: Berlin, West Germany, Springer-Verlag, 288 p.
- Egemeier, S. J., 1981, Cavern development by thermal waters: *National Speleological Society Bulletin*, v. 43, p. 31-51.
- Ewers, R. O., 1978, A model for the development of broadscale networks of groundwater flow in steeply dipping carbonate aquifers: *British Cave Research Association, Transactions*, v. 5, p. 121-125.
- 1982, An analysis of solution cavern development in the dimensions of length and breadth [Ph.D. thesis]: Hamilton, Ontario, McMaster University, 398 p.
- Ford, D. C., 1971, Geologic structure and a new explanation of limestone cavern genesis: *Cave Research Group of Great Britain, Transactions*, v. 13, p. 81-94.
- Ford, D. C., and Ewers, R. O., 1978, The development of limestone cave systems in the dimensions of length and depth: *Canadian Journal of Earth Sciences*, v. 15, p. 1783-1798.
- Ford, D. C., and Williams, P. W., 1989, Karst geomorphology and hydrology: London, England, Unwin Hyman, 601 p.
- Herman, J. S., and White, W. B., 1985, Dissolution kinetics of dolomite: Effects of lithology and fluid flow velocity: *Geochimica et Cosmochimica Acta*, v. 49, p. 2017-2026.
- Hess, J. W., and Harmon, R. S., 1981, Geochronology of speleothems from the Flint Ridge-Mammoth Cave System, Kentucky, USA: *International Congress of Speleology*, 8th, Bowling Green, Kentucky, Proceedings, p. 433-436.
- High, C. J., 1970, Aspects of the solutional erosion of limestone, with special consideration of lithological factors [Ph.D. thesis]: Bristol, U.K., University of Bristol, 228 p.
- Hill, C. A., 1987, Geology of Carlsbad Cavern and other caves in the Guadalupe Mountains, New Mexico and Texas: *New Mexico Bureau of Mines and Mineral Resources, Bulletin* 117, 150 p.
- Howard, A. D., and Howard, B. Y., 1967, Solution of limestone under laminar flow between parallel boundaries: *Caves and Karst*, v. 9, p. 25-38.
- Jennings, J. N., 1985, Karst geomorphology: Oxford, England, Basil Blackwell, 293 p.
- Kastning, E. H., 1977, Faults as positive and negative influences on groundwater flow and conduit enlargement, in Dilamarter, R. R., and Callany, S. C., eds., Hydrologic problems in karst regions: Bowling Green, Kentucky, Western Kentucky University, p. 193-201.
- Lauritzen, S.-E., Abbott, J., Arnesen, R., Crossley, G., Grepperud, D., Ive, A., and Johnson, S., 1985, Morphology and hydraulics of an active phreatic conduit: *British Cave Research Association, Transactions*, v. 12, p. 139-146.
- Mangin, A., 1975, Contribution à l'étude hydrodynamique des aquifères karstiques: *Annales de Spéléologie*, v. 29, p. 283-332, 495-601; v. 30, p. 21-124.
- McKnight, E. T., and Fischer, R. P., 1970, Geology and ore deposits of the Picher Field, Oklahoma and Kansas: *U.S. Geological Survey Professional Paper* 588, 165 p.
- Miotke, F.-D., and Palmer, A. N., 1972, Genetic relationship between caves and landforms in the Mammoth Cave National Park area: Würzburg, Germany, Böhler Verlag, 69 p.
- Morehouse, D. F., 1968, Cave development via the sulfuric acid reaction: *National Speleological Society Bulletin*, v. 30, p. 1-10.
- Morse, J. W., 1978, Dissolution kinetics of calcium carbonate in sea water: VI. The near-equilibrium dissolution kinetics of calcium carbonate-rich deep sea sediments: *American Journal of Science*, v. 278, p. 344-353.
- Myroie, J. E., 1988, Karst of San Salvador, in Myroie, J. E., ed., Field guide to the karst geology of San Salvador Island, Bahamas: *Mississippi State University, 10th Friends of Karst Meeting*, p. 17-44.
- Myroie, J. E., and Carew, J. L., 1987, Field evidence of the minimum time for speleogenesis: *National Speleological Society Bulletin*, v. 49, p. 67-72.
- Newson, M. D., 1971, The role of abrasion in cavern development: *Cave Research Group of Great Britain, Transactions*, v. 13, p. 101-107.
- Palmer, A. N., 1972, Dynamics of a sinking stream system, Onesquethaw Cave, New York: *National Speleological Society Bulletin*, v. 34, p. 89-110.
- 1975, The origin of maze caves: *National Speleological Society Bulletin*, v. 37, p. 56-76.
- 1981, Hydrochemical controls in the origin of limestone caves, in *International Speleological Congress*, 8th, Bowling Green, Kentucky, Proceedings, p. 120-122.
- 1984a, Geomorphic interpretation of karst features, in LaFleur, R. G., Groundwater as a geomorphic agent: Boston, Massachusetts, Allen and Unwin, p. 173-209.
- 1984b, Recent trends in karst geomorphology: *Journal of Geological Education*, v. 32, p. 247-253.
- 1984c, Objectives and current status of alpine and arctic karst research: *Norsk Geografisk Tidsskrift*, v. 38, no. 3-4, p. 145-150.
- 1987, Cave levels and their interpretation: *National Speleological Society Bulletin*, v. 49, p. 50-66.
- 1988, Solutional enlargement of openings in the vicinity of hydraulic structures in karst regions: 2nd Conference on Environmental Problems in Karst Terranes and their Solutions, Proceedings: Association of Ground Water Scientists and Engineers, p. 3-13.
- Palmer, A. N., Palmer, M. V., and Queen, J. M., 1977, Geology and origin of the caves of Bermuda, in *International Speleological Congress*, 7th, Sheffield, England, Proceedings, p. 336-339.
- Plummer, L. N., 1975, Mixing of sea water with calcium carbonate ground water: *Geological Society of America Memoir* 142, p. 219-236.
- Plummer, L. N., and Busenberg, E., 1982, The solubilities of calcite, aragonite, and vaterite in $\text{CO}_2\text{-H}_2\text{O}$ solutions between 0° and 90° C and an evaluation of the aqueous model for the system $\text{CaCO}_3\text{-CO}_2\text{-H}_2\text{O}$: *Geochimica et Cosmochimica Acta*, v. 46, p. 1011-1040.
- Plummer, L. N., and Wigley, T.M.L., 1976, The dissolution of calcite in CO_2 -saturated solutions at 25° C and 1 atmosphere total pressure: *Geochimica et Cosmochimica Acta*, v. 40, p. 191-202.
- Plummer, L. N., Vacher, H. L., MacKenzie, F. T., Bricker, O. P., and Land, L. S., 1976, Hydrochemistry of Bermuda: A case history of groundwater diagenesis of biocalcarenes: *Geological Society of America Bulletin*, v. 87, p. 1301-1316.
- Plummer, L. N., Wigley, T.M.L., and Parkhurst, D. L., 1978, The kinetics of calcite dissolution in CO_2 -water systems at 5° to 60° C and 0.0 to 1.0 atm CO_2 : *American Journal of Science*, v. 278, p. 179-216. Experimental data in National Auxiliary Publication Service Document 03209.
- Powell, R. L., 1970, Base level, lithologic and climatic controls of karst groundwater zones in south-central Indiana: *Indiana Academy of Science, Proceedings*, v. 79, p. 281-291.
- 1976, Some geomorphic and hydrologic implications of jointing in carbonate strata of Mississippian age in south-central Indiana [Ph.D. thesis]: Lafayette, Indiana, Purdue University, 169 p.
- Queen, J. M., 1981, A discussion and field guide to the geology of Carlsbad Caverns: Preliminary report to the National Park Service for the 8th International Speleological Congress, 64 p.
- Rauch, H. W., and White, W. B., 1977, Dissolution kinetics of carbonate rocks. I. Effects of lithology on dissolution rate: *Water Resources Research*, v. 13, p. 381-394.
- Rosenfeld, J. H., 1986, Kinetics of calcite dissolution in carbonic acid: *Cave Research Foundation, 1986 Annual Report*, p. 12-13.
- Schmidt, V. A., 1982, Magnetostratigraphy of sediments in Mammoth Cave, Kentucky: *Science*, v. 217, p. 827-829.
- Sjöberg, E. L., and Rickard, D. T., 1984, Temperature dependence of calcite dissolution kinetics between 1 and 62° C at pH 2.7 to 8.4 in aqueous solutions: *Geochimica et Cosmochimica Acta*, v. 48, p. 485-493.
- Smart, C. C., 1988, A deductive model of karst evolution based on hydrological probability: *Earth Surface Processes and Landforms*, v. 13, p. 271-288.
- Smith, D. I., and Atkinson, T. C., 1976, Process, landforms, and climate in limestone regions, in Derbyshire, E., ed., *Geomorphology and climate*: New York, Wiley, p. 367-409.
- Swinnerton, A. C., 1932, Origin of limestone caverns: *Geological Society of America Bulletin*, v. 43, p. 663-694.
- Takács-Bolner, K., and Kraus, S., 1989, The results of research into caves of thermal water origin: *Karst es Barlang, Hungarian Speleological Society Bulletin*, special issue for 10th International Speleological Congress, p. 31-38.
- Thraill, J., 1968, Chemical and hydrologic factors in the excavation of limestone caves: *Geological Society of America Bulletin*, v. 79, p. 19-46.
- Thraill, J., and Robl, T. L., 1981, Carbonate geochemistry of vadose water recharging limestone aquifers: *Journal of Hydrology*, v. 54, p. 195-208.
- Wagman, D. D., Evans, W. H., Parker, V. B., Schumm, R. H., Harlow, I., Bailey, S. M., Churney, K. L., and Nutall, R. L., 1982, The NBS tables of chemical thermodynamic properties: Selected values for inorganic and C1 and C2 organic substances in SI units: *Journal of Physical Chemistry, Reference Data* 11, Supplement 2, p. 1-392.
- Warwick, G. T., 1968, Some primitive features in British caves, in *International Speleological Congress*, 4th, Ljubljana, Yugoslavia, Proceedings, p. 239-252.
- White, W. B., 1969, Conceptual models for carbonate aquifers: *Ground Water*, v. 7, p. 15-21.
- 1977a, Conceptual models for carbonate aquifers, revisited, in Dilamarter, R. R., and Callany, S. C., eds., *Hydrologic problems in karst regions*: Bowling Green, Kentucky, Western Kentucky University, p. 176-187.
- 1977b, Role of solution kinetics in the development of karst aquifers, in Tolson, J. S., and Doyle, F. L., eds., *Karst hydrogeology: Congress of the International Association of Hydrogeologists*, 12th, Memoirs, p. 503-517.
- 1988, Geomorphology and hydrology of karst terrains: New York, Oxford University Press, 464 p.
- Wigley, T.M.L., and Plummer, L. N., 1976, Mixing of carbonate waters: *Geochimica et Cosmochimica Acta*, v. 40, p. 989-995.
- Williams, P. W., 1985, Subcutaneous hydrology and the development of doline and cockpit karst: *Zeitschrift für Geomorphologie*, v. 29, p. 463-482.
- Wood, W. W., and Petraitis, M. J., 1984, Origin and distribution of carbon dioxide in the unsaturated zone of the southern High Plains: *Water Resources Research*, v. 20, p. 1193-1208.

MANUSCRIPT RECEIVED BY THE SOCIETY NOVEMBER 13, 1989
 REVISED MANUSCRIPT RECEIVED MAY 28, 1990
 MANUSCRIPT ACCEPTED JUNE 18, 1990